https://doi.org/10.5194/bg-2020-227
Preprint. Discussion started: 3 July 2020

Biogeosciences
Discussions
Open Access
EGU

Photodegradation and biodegradation of dissolved organic matter on the surface of the Greenland Ice Sheet

Miranda J. Nicholes[1], Christopher Williamson[1], Martyn Tranter[1], Alexandra Holland[1], Marian Yallop[2], Alexandre Anesio[3]

[1]Bristol Glaciology Centre, School of Geographical Sciences, University of Bristol, Bristol, BS8 1SS, UK
[2]School of Biological Sciences, University of Bristol, Bristol, BS8 1TQ, UK
[3]Department of Environmental Science, Aarhus University, Roskilde, 4000, Denmark

Correspondence to: Miranda Nicholes (miranda.nicholes@bristol.ac.uk)

Abstract

The surface (supraglacial) environment of the Greenland Ice Sheet (GrIS) is an active site for the storage, transformation and transport of carbon, which is driven by extremely high levels of solar radiation throughout the ablation season. Within the south west of the GrIS, blooms of Streptophyte micro-algae (hereafter 'glacier algae') at abundances of ~ 10^5 cell mL^{-1} dominate primary production in the surface ice and provide dissolved organic matter (DOM) to the heterotrophic bacterial community. Glacier algae contain photoprotective secondary phenolic pigment that comprises a large proportion of the cell (~ 4 % of the dry weight) and could represent a substantial, additional carbon source for the heterotrophic community. The transformation and degradation of DOM by solar radiation (photodegradation) and heterotrophic communities (biodegradation) represent two crucial controls on DOM composition and quantity; however, the influence of these processes within the surface ice is yet to be constrained. This study therefore assessed responses in the composition and quantity of two carbon sources (glacier algae secondary pigment and surface ice DOM) following exposure to UV, PAR, UV+PAR (photodegradation) and subsequent incubation with bacterial communities isolated from the ambient environment (biodegradation). Our results indicate that exposure to predominantly UV radiation altered the composition of glacier algal pigment and surface ice DOM; however, the quantity of DOM remained constant. Biodegradation caused the greatest changes to both DOM composition and quantity, particularly in surface ice DOM. Secondary pigment extracted from glacier algae was not a highly bioavailable source of carbon and did not support significant growth of surface ice heterotrophic bacterial communities. Conversely, low molecular weight compounds in surface ice DOM were rapidly utilised by heterotrophic bacteria supporting between a 3 and 9-fold increase in bacterial abundance over a 30-day incubation. We found that photodegradation of glacier algal pigment and surface ice DOM did not influence heterotrophic consumption. Photodegradation and biodegradation of DOM in the surface ice habitat are likely intimately linked and act as fundamental controls on the composition and quantity of DOM exported to downstream environments.

1 Introduction

Dissolved organic matter (DOM) is ubiquitous across all aquatic systems and comprises a chemically diverse range of compounds (Baker and Spencer, 2004; Coble et al., 2014; Kellerman et al., 2018). DOM has multiple

https://doi.org/10.5194/bg-2020-227
Preprint. Discussion started: 3 July 2020

functions within ecosystems including the provision of substrates for heterotrophic organisms; mobilising organic and inorganic pollutants; and influencing the bioavailability of nutrients (Aiken, 2014; Baker and Spencer, 2004). DOM originates from either autochthonous (i.e. in situ production) or allochthonous (i.e. terrestrial) sources with varying levels of reactivity and composition. For example, autochthonous DOM typically comprises of low molecular weight (LMW) compounds such as amino acids and carbohydrates, which are highly bioavailable (Amado et al., 2015; Murphy et al., 2008; Stedmon and Markager, 2005). In contrast, allochthonous carbon usually comprise of high molecular weight (HMW), aromatic compounds of a more recalcitrant nature (Amado et al., 2015; Murphy et al., 2008). The composition and quantity of DOM fundamentally controls the flow of carbon and energy through aquatic ecosystems, shaping the structure of the food web.

The composition and quantity of DOM in aquatic ecosystems is primarily controlled by two processes: photodegradation and biodegradation (Benner and Kaiser, 2011; Fasching et al., 2014; Hansen et al., 2016). Chromophoric DOM (CDOM) comprises a proportion of total DOM that is highly reactive on exposure to solar radiation (Coble, 2007). Consequently, high energy ultra-violet (UV) radiation can strongly influence carbon cycling by degrading CDOM into a range of species including dissolved inorganic carbon, smaller organic carbon compounds and reactive oxygen species (ROS; e.g. hydroxyl radicals) (Coble, 2007; Lindell et al., 1995; Stefan et al., 2000; Tranvik and Bertilsson, 2001). DOM is a vast resource of biologically available organic carbon that is consumed and transformed by heterotrophic bacteria (biodegradation) (Fellman et al., 2010). Carbon is utilised by heterotrophic bacteria through two different processes: i) complete mineralisation of carbon to obtain energy i.e. respiration; ii) incorporation into microbial biomass (Ducklow, 2000). Photodegradation of DOM can strongly influence the interaction between heterotrophic communities and carbon within ecosystems exposed to high levels of solar radiation (Anesio and Granéli, 2004; Stefan et al., 2000; Tranvik and Bertilsson, 2001; Tranvik and Kokalj, 1998). The photodegradation of complex, recalcitrant DOM into more bioavailable compounds has been found to stimulate bacterial production (Amado et al., 2015; Lindell et al., 1995; Zepp and Moran, 1997); however, radiation can also remove LMW, bioavailable compounds from the DOM pool (Tranvik and Kokalj, 1998). Additionally, the generation of ROS via photodegradation damages bacteria, reducing production (Holzinger and Lütz, 2006; Ravanat et al., 2001). It is thought that the relative influence of photodegradation on bacterial production is determined by the balance of these processes and relates to the source of DOM; i.e. photodegradation tends to reduces bioavailability of algal-derived DOM but increases bioavailability of allochthonous DOM (Amado et al., 2015). Thus, in ecosystems exposed to high levels of solar radiation, DOM composition and quantity is controlled by two highly interlinked processes.

The surface ice of the Greenland Ice Sheet (GrIS) hosts abundant and active algal and bacterial communities which influence both regional and global carbon cycling (Nicholes et al., 2019; Perini et al., 2019; Williamson et al., 2018; Yallop et al., 2012). During the ablation season, the surface ice is exposed to extreme levels of photosynthetically active radiation (PAR; ~ 1700 µmol photons m^{-2} s^{-1} on a cloudless day) and UV radiation. Solar radiation drives high levels of carbon fixation (0.35 – 1.12 mg C L^{-1} d^{-1}) predominantly by blooms of highly pigmented glacier algae (Musilova et al., 2017; Williamson et al., 2018; Yallop et al., 2012) that are particularly prevalent in the so-called 'Dark Zone' in the south west of the ice sheet. Glacier algae are well-adapted to the extreme light conditions and synthesise an abundant secondary phenolic pigment (purpurogallin carboxylic acid-

https://doi.org/10.5194/bg-2020-227
Preprint. Discussion started: 3 July 2020


Biogeosciences
Discussions
Open Access
EGU

6-*O*-β-D-glucopyranoside) that exhibits maximal absorbance in UV-B wavelengths and thus protects the cells from photo-damage (Remias et al., 2012; Williamson et al., 2020). This pigment comprises a relatively high proportion of glacier algal cellular content (~ 4 % of the dry weight; Williamson et al. 2020) and likely reaches high concentrations during bloom events when algal abundance peaks at 10^4 cells mL^{-1} (Williamson et al., 2018; Yallop et al., 2012). Glacier algal pigment, comprised predominantly of phenolic based compounds (Remias et al., 2012), could therefore represent a vast source of organic carbon within the GrIS supraglacial environment if released during cell lysis due to natural senescence or viral infection, providing an important energy source for the diverse and active bacterial communities that numerically dominate surface ice (Hodson et al., 2008; Nicholes et al., 2019; Stibal et al., 2015). These communities are thought to utilise predominantly algal-derived DOM to achieve rates of bacterial production (BP) ranging 0.03 – 0.6 µg C L^{-1} h^{-1} (Nicholes et al., 2019; Yallop et al., 2012); approximately 30-times less than primary production (Nicholes et al., 2019; Yallop et al., 2012).

Despite the presence of active autotrophic and heterotrophic communities, there remains several critical knowledge gaps regarding carbon cycling within the high-light supraglacial surface ice environment. These include the potential impact of photodegradation on surface ice DOM and subsequent heterotrophic utilisation; the susceptibility of glacier algal secondary phenolic pigment to photodegradation (given its maximum absorbance in UV-B wavelengths) and its bioavailability to heterotrophic bacteria; and the components of surface ice DOM that are degraded by heterotrophic bacteria. Thus far, investigations into DOM cycling in glacial environments have revealed that photodegradation produces a slight increase in bioavailable DOM in Antarctic snow samples (Antony et al., 2018). However, DOM biodegradation was found to produce photoreactive compounds highlighting the interlinked nature of these two processes (Antony et al., 2017, 2018). Here, we hypothesise that photodegradation may alter the composition and bioavailability of organic carbon to heterotrophic bacterial communities, subsequently impacting biodegradation pathways in surface ice. This investigation therefore aimed to constrain changes in the composition and quantity of both ambient surface ice DOM and glacier algae secondary phenolic pigment (representing a potentially abundant and refractory DOM source) following exposure to UV and PAR radiation, and their subsequent bioavailability to surface ice bacterial communities.

2 Methodology

An incubation experiment was conducted to determine the degree to which glacier algal phenolic pigment (hereafter 'pigment') and surface ice dissolved organic matter (DOM) degrade when exposed to combinations of ultraviolet (UV) and photosynthetically active radiation (PAR) radiation. The bioavailability of pigment and surface ice DOM following photodegradation was subsequently assessed via incubations with a heterotrophic bacterial community isolated from surface ice samples.

2.1 Surface ice preparation

Surface ice was obtained during the 2017 Black and Bloom field campaign (31st May to 1st July 2017) from the primary ice camp established within the GrIS ablation zone approximately 35 km from the south-western ice sheet margin (67 °04'43.3" N, 49 °20'29.7" W), adjacent to the S6 PROMICE weather station. The top 2cm of surface

https://doi.org/10.5194/bg-2020-227
Preprint. Discussion started: 3 July 2020

ice containing a high algal coverage (~ 10^4 cells mL^{-1}) (Williamson et al., 2018) was sampled using a clean ice saw and transferred into 5 WhirlPak bags. Each WhirlPak bag contained approximately 1.5L of frozen surface ice and was transported back to the University of Bristol and stored at -20 ºC. Prior to photodegradation, surface ice was thawed over 24 hours at 3 ºC and filtered through a 0.2 µm polyethersulfone (PES) filter (pre-flushed with 50 mL Milli-Q) to remove bacteria, fungi and glacier algae. The filtrate was homogenised and decanted into 250 mL pre-combusted Pyrex crystallising basins (n = 20).

2.2 Glacier algal pigment preparation

Secondary phenolic pigment was extracted from glacier algal cells present in surface ice sampled from the primary ice camp as outlined previously. Between 100 - 200 mL of sample (n = 45) was filtered onto combusted GF/F filters, frozen and transported to the University of Bristol. Filters were freeze-dried for 24 hours and water-soluble pigments extracted in 5 mL of Milli-Q water, following Remias *et al.*, (2012) and Williamson *et al.*, (2018). A phase separation with n-hexane was performed to remove non-polar constituents from the raw extract, which was subsequently stored frozen at -20 ºC until being defrosted over 12 hours prior to use. Pigment was added to Milli-Q water to a 1:100 v/v dilution, homogenised and divided into 250 mL pre-combusted Pyrex crystallising basins (n = 20).

2.3 Photodegradation

To stimulate photodegradation in the pigment and surface ice, both carbon sources were exposed to combinations of UV and PAR over a 48-hour period. Short-wavelength, high-energy UV-radiation is widely reported as responsible for inducing photodegradation in aquatic ecosystems (Amado et al., 2015; Bertilsson and Tranvik, 1998; Stefan et al., 2000; Tranvik and Bertilsson, 2001). Ultra-violet bulbs (25W, 220-240V, Exo Terra, Canada) and LED bulbs (Prolite, UK) were used to create 3 different light treatments: UV, PAR (432 µmol photons m^{-2} s^{-1}) or UV plus PAR (UV+PAR). Pigment and surface ice were exposed to UV, PAR and UV+PAR (n = 5 per light treatment per carbon source) at 3 ºC for 48 hours. Light exposure for 48 hours produced 840 kJ m^{-2} of UV-A, 412 kJ m^{-2} of UV-B and 16,456 kJ m^{-2} of PAR, equivalent to approximately 2, 10 and 4 days of exposure on the surface of the GrIS respectively (https://pvlighthouse.com.au/). To serve as a control, pigment and surface ice samples were wrapped in foil and kept in total darkness during the exposure period ("DARK", n = 5). In addition, a Milli-Q control (n = 5 per light treatment) was incubated alongside pigment and surface ice to detect any contamination. Following photodegradation, dissolved organic matter composition (UV-Vis and fluorescence spectroscopy) and quantity (dissolved organic carbon concentration) was assessed.

2.4 Biodegradation

To determine the bioavailability of photodegraded pigment and surface ice, carbon sources were inoculated with bacteria and incubated for 31 days. Bacterial cultures were established from surface ice from the primary ice camp, sampled as outlined previously. The surface ice was thawed at 3 ºC over 48 hours, decanted into a pre-combusted 1000 mL beaker, covered with furnaced foil and sonicated for 2 minutes to facilitate cell detachment

https://doi.org/10.5194/bg-2020-227
Preprint. Discussion started: 3 July 2020


Biogeosciences
Discussions
Open Access
EGU

from particles (Bradley et al., 2016). To isolate bacteria, surface ice was filtered through a combusted GF/D filter (Whatman, USA) and stored at 3 ºC. Bacteria were inoculated to pigment, surface ice and Milli-Q control at a 10 % v/v final concentration in pre-combusted 30 mL amber glass vials, maintaining a headspace. Bacterial abundance at the start of the incubation averaged $3.7 \pm 0.2 \times 10^4$ cells mL^{-1} and did not differ significantly across pigment, surface ice or Milli-Q control samples.

To control for and examine the potential influence of nutrient limitation on carbon consumption and modification during incubations, half of all replicates received additions of inorganic nitrogen (NH_4NO_3) and phosphorus (KH_2PO_4) across all treatments at final concentrations of 30 µM L^{-1} and 10 µM L^{-1}, respectively; representing 10-times ambient concentrations reported from the surface of the GrIS (< 1 µM P L^{-1} Hawkings *et al.*, 2016; 1.3 µM DIN L^{-1} Wadham *et al.*, 2016). Incubations proceeded at 3 ºC in the dark for a period of 31 days, with destructive sampling at days 0, 3, 6, 10, 17 and 31 to assess biodegradation impacts to DOM composition and quantity within incubations, relative to bacterial abundance and biovolume.

2.5 UV-Vis spectroscopy

Analysis of CDOM via spectroscopy can provide information regarding DOM aromaticity, sources and reactivity (Li and Hur, 2017). Accordingly, UV-Vis spectroscopy of the pigment and surface ice was conducted following both photodegradation and biodegradation steps of our experiment. Absorbance spectra were obtained using a Varian Cary 60 UV/Vis spectrophotometer (Agilent Technologies, USA) with scans run over wavelengths ranging from 200 – 800 nm at 2 nm intervals. Absorption data is expressed as absorption coefficients, calculated following Eq. (1):

$$a(\lambda) = 2.303\, A(\lambda)/l \quad (1)$$

where $a(\lambda)$ is absorption coefficient (m^{-1}), $A(\lambda)$ is the raw absorbance and l is the cuvette pathlength (m). Absorbance indices utilised are summarised in Table 1. Specific ultraviolet absorbance at 280 nm ($SUVA_{280}$) is a proxy for total aromaticity as electron transition occurs within this absorbance region for phenolic arenes, benzoic acids, aniline derivatives, polyenes and polycyclic aromatic hydrocarbons with two or more rings (Uyguner and Bekbolet, 2005). Although SUVA indices give an indication of the relative proportion of aromatic DOM, the relative reactivity of these compounds cannot be inferred (Weishaar et al., 2003). We therefore combined UV-Vis and fluorescence spectroscopy to provide information of composition and bioavailability of DOM.

2.5.1 Fluorescence spectroscopy

A small fraction of CDOM, known as fluorescent DOM (FDOM), emits fluorescence energy when excited by photons at specific energies (Li and Hur, 2017). Fluorescence spectroscopy therefore characterises FDOM providing information on source, reactivity and composition (Aiken, 2014; Coble, 1996; Coble et al., 1990, 2014). To minimise the effects of temperature, samples were left to reach room temperature before measurements were undertaken. Fluorescence scans were conducted using a Varian Cary Eclipse Fluorescence Spectrophotometer (Agilent Technologies, USA) scanning over excitation wavelengths 250 – 450 nm at 5 nm intervals and 300 –

https://doi.org/10.5194/bg-2020-227
Preprint. Discussion started: 3 July 2020

600 nm emission wavelengths at 2 nm intervals. Excitation- Emission Matrices (EEMs) were processed using the StaRdom package (Pucher et al., 2019) in R (R Development Core Team, 2019). EEMs were blank corrected using EEMs from daily Milli-Q scans, corrected for inner-filter effects using absorbance scans and Raman normalised. Fluorescence indices derived from EEMs are summarised in Table 1. The fluorescence intensity of commonly identified peaks in natural waters, summarised in Table 2, was identified in sample EEMs.

https://doi.org/10.5194/bg-2020-227
Preprint. Discussion started: 3 July 2020

195 **Table 1: Absorbance and fluorescence indices utilised in this study. LMW= low molecular weight. Adapted from**
196 **Hansen et al., (2016)**

Indices	Calculation	Proxy	Reference
Specific ultraviolet absorption (SUVA) E.g. $SUVA_{254}$, $SUVA_{280}$, $SUVA_{365}$ (L mg^{-1} m^{-1})	Absorption coefficient at given wavelength in the ultraviolet region divided by DOC concentration	A higher number is generally associated with greater aromatic DOC content	(Weishaar et al., 2003)
Specific visible absorption (SVA) E.g. SVA_{440} (L mg^{-1} m^{-1})	Absorption coefficient at 440 nm divided by DOC concentration	A higher number is generally associated with greater aromatic DOC content	(Chin et al., 1994)
Absorption coefficient at 440 nm (A_{440}) (m^{-1})	Absorption coefficient at 440 nm	Indicates the colour and is therefore a proxy for concentration of humic acid	(Fasching et al., 2014)
Spectral slope λ300-700 nm ($S_{300-700}$) (nm^{-1})	Spectral slope within log-transformed spectra between 300 and 700 nm	Generally a higher value indicates LMW and/or decreasing aromaticity	(Helms et al., 2008)
Humification index (HIX)	The area under the emission spectra 435-480 nm divided by the peak area 300-345 nm + 435 – 480 nm, at excitation wavelength 254 nm	Gives an indication of the degree of humification. Higher values indicate an increasing degree of humification	(Ohno, 2002)
Fluorescence index (FI)	The ratio of emission wavelengths at 470 nm and 520 nm, obtained at an excitation wavelength of 370 nm	Identified the relative contribution of terrestrial and microbial sources to the DOM pool. Increasing values suggests a microbial source	(McKnight et al., 2001)

197

https://doi.org/10.5194/bg-2020-227
Preprint. Discussion started: 3 July 2020

198 **Table 2: Summary of commonly identified fluorescence peaks of aquatic DOM adapted from Fellman, Hood and**
199 **Spencer, (2010). Peaks were originally identified by Coble et al., (1990), (2014); Coble, (1996); Coble, Del Castillo and**
200 **Avril, (1998); Murphy et al., (2008). HMW = high molecular weight; LMW = low molecular weight.**

Peak name	Excitation (ex) and emission (em) maxima (nm)	Associated component	Possible sources
B	ex 270 - 275, em 304 - 312	Tyrosine-like (proteinaceous)	Terrestrial, autochthonous production, microbial processing
T	ex 270 - 280, em 330 - 368	Tryptophan-like (proteinaceous)	Terrestrial, autochthonous production, microbial processing
M	ex 290 - 325, em 370 - 430	UVA humic-like. LMW, common in marine environments and associated with biological activity	Terrestrial, autochthonous production, microbial processing
A	ex < 260, em 448 - 480	UVC humic-like. Often HMW and aromatic	Terrestrial
C	ex 320 - 360, em 420 - 460	UVC humic-like. Often HMW and aromatic	Terrestrial

201

202 **2.6 Dissolved organic carbon concentration**

203 Dissolved organic carbon (DOC) concentration was measured following photodegradation and biodegradation
204 steps to determine the influence of these processes on the total quantity of carbon available. Samples were filtered
205 through a pre-flushed (3 times with 10 mL of Milli-Q) 0.22 µm polyethersulfone (PES) syringe filter (Whatman,
206 England) into acid washed 30 mL HDPE Nalgene bottles and frozen until analysis. DOC concentrations were
207 quantified using a Shimadzu TOC-L Organic Carbon Analyser with a high-sensitivity catalyst. Non-purgeable
208 organic carbon (NPOC) was measured following the acidification of samples with hydrochloric acid and catalytic
209 combustion (680ºC) of DOC to carbon dioxide, which is subsequently measured by infrared absorption. The limit
210 of detection (LoD) was 67 µg L^{-1} with a precision of ± 3 % and an accuracy of ± 2 % as defined by the comparison
211 of a gravimetrically diluted 500 mg L^{-1} TOC certified stock standard to a concentration of 500 µg L^{-1} (Sigma
212 TraceCERT). Procedural blanks were analysed alongside samples to monitor for any contamination which may
213 have been introduced at any stage during the incubation and processing procedures. The DOC concentration
214 decreased by ~ 24 % in the control (Milli-Q inoculated with bacteria) and DOC concentrations in the pigment and
215 surface ice were therefore normalised against the control. The percent of biodegradable or bioavailable DOC

https://doi.org/10.5194/bg-2020-227
Preprint. Discussion started: 3 July 2020

(%BDOC) was calculated as the difference in DOC concentration at the start and end of the 31 day biodegradation incubation period (Fasching et al., 2014).

2.7 Bacterial enumeration and biomass

Bacterial enumeration was conducted at 0, 6, 15 and 30 days from 300 µL of sample (n = 3) by epifluorescence microscopy following staining with 4', 6-diamidino-2-phenylindole (DAPI, Sigma) at a final concentration of 10 µg mL^{-1} (Porter and Feig, 1980). The staining, filtering and mounting procedure was conducted as outlined by Bradley *et al.* (2016). Bacterial cells were counted using a Leica DM 2000 epifluorescence microscope at 1000x magnification with attached MC120 HD microscope camera (Leica, Germany). A minimum of 300 cells or 30 randomly selected grids (each 10^4 μm^2) were counted. Abundance in the pigment and surface ice was normalised to the control (Milli-Q inoculated with bacteria).

Imaging for the estimation of cell volumes was performed in parallel and measurements of cell diameter and height made using ImageJ software. Cell volumes were calculated following Eq. (2):

$$V = (w^2 * \pi/4) * (l - w) + (\pi * w^3/6), \quad (2)$$

where V (μm^3) is the cell volume, and w and l are cell width and length (in µm) (Fasching et al., 2014). Estimated cell volumes were converted to individual cell carbon content according to Bratbak and Dundas (1984). Microbial biomass was then calculated as the product of bacterial abundance and the individual cell carbon content for each sample. Bacterial growth efficiency (BGE) is an indicator of the use of DOM for bacterial growth and gives an indication of the flow of carbon through the bacterial biomass (Anesio et al., 2005; Del Giorgio and Cole, 1998). BGE was estimated as the change in biomass divided by the change in DOC concentration (assumed to represent the DOC incorporated into the bacterial biomass plus respiration) over the 31-day incubation period. This assumes carbon incorporated into the bacterial biomass was not utilised for respiration.

2.8 Data analysis

All statistical analyses and plotting of data were performed using R v.3.4.1 (R Core Team, 2019). Prior to parametric analysis of datasets, Shapiro-Wilks Test combined with interrogation of frequency histograms was used to determine normality. Three-way analysis of variance (ANOVA) with the fixed factors of carbon source (i.e. pigment or surface ice; 2 levels); light (4 levels) and degradation type (i.e. photodegradation or biodegradation; 2 levels) was used to determine significant differences in the absorbance and fluorescence indices. Principal Component Analysis (PCA) was also used to summarise normalised and centred absorbance and fluorescence indices utilising the 'factoextra' R package (Kassambara, 2020). Differences within DOC concentration and bacterial abundance were described using a three-way ANOVA with the fixed factors of 'time' (4 levels), 'light' (4 levels), nutrients (i.e. normal or +nutrients; 2 levels) for the pigment and surface ice.

https://doi.org/10.5194/bg-2020-227
Preprint. Discussion started: 3 July 2020


Biogeosciences
Discussions
Open Access
EGU

3 Results

3.1 DOM composition

3.1.1 UV-Vis absorbance properties

Glacier algal pigment DOM that was not exposed to radiation (DARK) displayed two prominent peaks in absorption at λ_{285nm} and λ_{304nm} as well as a secondary peak at λ_{385nm} (Figure 1). These peaks were also evident in pigment exposed to PAR and UV+PAR, which exhibited spectra highly comparable to DARK. In contrast, UV-irradiated pigment revealed marked differences in absorption with a conspicuous depression in the peaks at λ_{285nm} and λ_{304nm} and 10 % greater absorption at λ_{250nm} and between $\lambda_{325 - 600nm}$. This was reflected in average specific UV absorbance (SUVA) indices (Table 3) for UV-irradiated pigment which were 0.9 L m^{-1} mg^{-1} lower than DARK for $SUVA_{280}$ and between 0.8 - 1.0 L m^{-1} mg^{-1} higher for $SUVA_{254}$ and $SUVA_{365}$. For all light treatments, absorption decreased with increasing wavelength across visible wavelengths (400 – 700 nm). Average absorption at 440 nm (A_{440}) was 16.9 ± 0.7 m^{-1} in DARK and did not differ significantly across light treatments.

The inoculation of DARK pigment with bacteria (biodegradation) resulted in pronounced differences in the absorbance spectra. For example, a conspicuous 33 % depression was evident in the peaks at λ_{285nm} and λ_{304nm} and the peak at λ_{385nm} was absent. In addition, a secondary peak at λ_{330nm} developed which was not evident in the initial DARK spectra. $SUVA_{254}$ and $SUVA_{365}$ indices were significantly higher following biodegradation whereas $SUVA_{280}$ was significantly lower ($F_{3,32}$ = 21.8, $p < 0.001$; $F_{3,32}$ = 20.0, $p < 0.001$; $F_{3,32}$ = 36.3, $p < 0.001$ respectively). Spectral differences across light treatments were also apparent following biodegradation with the largest deviations in absorption occurring within UV wavelengths (200 – 400 nm). In particular, UV-irradiated pigment retained the greatest absorption at λ_{285nm} and λ_{304nm} therefore $SUVA_{280}$ for this treatment was significantly larger than DARK ($F_{3,32}$ = 1.7, $p < 0.01$). All light treatments exhibited an ~ 20 % increase in A_{440} following biodegradation.

https://doi.org/10.5194/bg-2020-227
Preprint. Discussion started: 3 July 2020

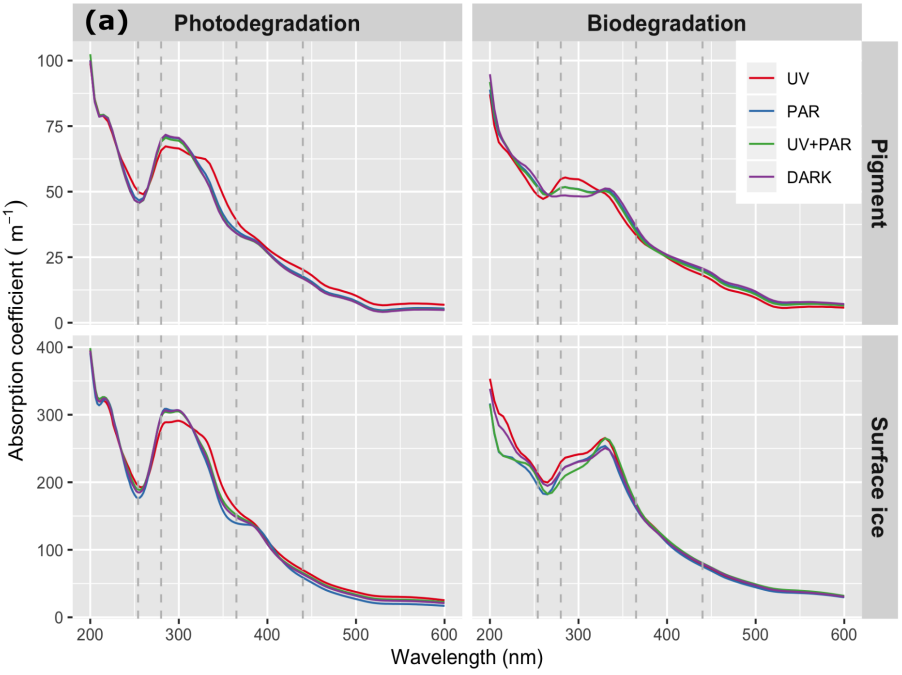

Figure 1: Average (a) and first derivative (b) of absorbance spectra across light treatments for the pigment and surface ice after exposure to light regimes (photodegradation) and following 31 days incubation with bacteria (biodegradation) (n=3). Dashed lines indicate the wavelengths at which specific UV absorbance (SUVA) was calculated (254 nm, 280 nm, 365 nm) and the absorbance at 440 nm (A_{440}).

https://doi.org/10.5194/bg-2020-227
Preprint. Discussion started: 3 July 2020

Biogeosciences Discussions Open Access EGU

Table 3: Specific UV absorbance values (L m^{-1} mg^{-1}) at 254 nm (SUVA254), 280 nm (SUVA280) and 365 nm (SUVA365) following photodegradation (Photo) and biodegradation (Bio) for the pigment and surface ice (mean ± SE, n=3). Highlighted values reflect trends on the absorbance spectra outlined previously. No significant differences were identified across light treatments per degradation type (i.e. photodegradation or biodegradation) per carbon source (pigment or surface ice), apart from $SUVA_{280}$ indices for pigment. Letters to denote homogenous subsets (lower case) are only displayed for this exception. Upper case letter denote significant differences between photodegradation and biodegradation per light treatment per carbon source.

DOM source	Light treatment	$SUVA_{254}$		$SUVA_{280}$		$SUVA_{365}$	
		Photo	Bio	Photo	Bio	Photo	Bio
Pigment	UV	**9.8 ± 0.2**^{A}	12.5 ± 0.7 ^{A}	**12.9 ± 0.2**^{A}	^{a}14.2 ± 0.7 ^{A}	**7.7 ± 0.1**^{A}	8.6 ± 0.7^{B}
	PAR	9.2 ± 0.1^{A}	13.4 ± 0.4 ^{A}	13.8 ± 0.1^{A}	^{ac}13.4 ± 0.3 ^{A}	7.0 ± 0.1^{A}	9.2 ± 0.5^{B}
	UV + PAR	9.1 ± 0.3^{A}	10.9 ± 0.3^{A}	13.7 ± 0.3^{A}	^{bc}11.0 ± 0.1^{B}	6.8 ± 0.4^{A}	7.4 ± 0.3^{B}
	Dark	9.0 ± 0.2^{A}	12.9 ± 0.4 ^{A}	13.8 ± 0.2^{A}	^{c}11.7 ± 0.1^{B}	6.7 ± 0.2^{A}	8.9 ± 0.6^{B}
Surface ice	UV	**9.0 ± 0.4**^{A}	13.2 ± 0.2^{B}	**12.9 ± 0.6**^{A}	14.5 ± 0.3^{A}	**7.4 ± 0.5**^{A}	10.5 ± 0.3^{A}
	PAR	**8.1 ± 0.6**^{A}	12.8 ± 0.3^{B}	13.7 ± 0.6^{A}	14.4 ± 0.3^{A}	6.4 ± 0.7^{A}	10.7 ± 0.3^{B}
	UV + PAR	8.7 ± 0.1^{A}	13.3 ± 0.4^{B}	13.6 ± 0.1^{A}	13.3 ± 0.2^{A}	7.0 ± 0.2^{A}	11.1 ± 0.4^{A}
	Dark	8.4 ± 0.2^{A}	14.1 ± 0.1^{B}	13.8 ± 0.2^{A}	14.8 ± 0.8^{A}	6.8 ± 0.2^{A}	11.2 ± 0.3^{A}

DARK surface ice DOM exhibited absorption on average ~ 4 times greater than the DARK pigment DOM (Figure 1); however, distinct similarities in absorption were evident, particularly the corresponding peaks at λ_{285nm}, λ_{304nm} and λ_{385nm}. The average A_{440} was 62.6 ± 2.4 m^{-1} which was 3 times larger than the DARK pigment. Photodegraded surface ice exhibited spectral differences, with the most striking disparities in the UV and PAR treatments. In particular, surface ice exposed to UV radiation exhibited ~ 5 % less absorption at λ_{304nm} and an average $SUVA_{280}$ 1.1 L m^{-1} mg^{-1} lower than DARK (Table 3). Equally, PAR-irradiated surface ice exhibited lower absorption at λ_{250nm} and $\lambda_{350-370nm}$ and subsequently the average $SUVA_{254}$ was 5 % lower than DARK.

The biodegraded DARK surface ice absorption spectra exhibited similar trends to the pigment with a ~ 20 % depression in peaks at λ_{285nm} and λ_{304nm}; however, retained more defined peaks at these wavelengths compared to the DARK pigment. In addition, a much more pronounced secondary peak at λ_{330nm} was visible in the DARK surface ice. Although $SUVA_{254}$ in the DARK treatment increased significantly by 65 % following biodegradation ($F_{3,32} = 21.8$, $p < 0.001$), the other SUVA indices were not significantly different. Deviations in the spectra across light treatments is largely confined between $\lambda_{200-350nm}$, with UV exhibiting the largest absorption over these wavelengths and UV and UV+PAR the lowest. Absorbance across visible wavelengths was highly consistent across light treatments and a ~ 20 % increase A_{440} was evident following biodegradation.

https://doi.org/10.5194/bg-2020-227
Preprint. Discussion started: 3 July 2020

Biogeosciences
Discussions
Open Access
EGU

306 **3.1.2 Fluorescence properties**

307 Peaks commonly identified in the fluorescence spectra of natural waters (B, T, M, A, C) (Coble, 1996; Coble et
308 al., 2014) were all present in the DARK pigment treatment (Figure 2; Figure 3). We observed an approximate
309 50:50 ratio between peaks associated with fluorophores in proteinaceous (B and T) and humic-like (A, C and M)
310 DOM in the DARK treatment. Following photodegradation of the pigment, the relative intensity of all peaks was
311 comparable with DARK and only a slight increase in peak A was observed in the PAR treatment. Biodegradation
312 was observed to alter the fluorescence signature of the pigment with humic-like fluorescence increasing by almost
313 25 % in the DARK treatment. UV and UV+PAR-irradiated pigment resulted in very little difference in
314 fluorescence intensities compared to DARK. Only the PAR treatment exhibited noticeable changes with ~ 10 %
315 greater fluorescence of peak B and a similar decrease in peak A compared to DARK.
316
317 In contrast to the pigment, DARK surface ice was dominated by fluorescence associated with humic-like DOM
318 (> 75 %) consisting predominantly of peaks A and C. Following photodegradation, the relative intensity of peaks
319 deviated between light treatments. For example, the fluorescence intensities of humic-like peaks (A and C) was ~
320 12 % lower in the UV treatment compared to DARK. In addition, PAR and UV+PAR exposed surface ice did not
321 contain peak T fluorescence but exhibited almost double the fluorescence associated with peak M. The
322 biodegradation of surface ice resulted in an ~ 10 % increase in fluorescence associated with humic-like DOM in
323 the DARK treatment. Reductions in proteinaceous fluorescence in DARK was particularly evident for peak B
324 which was almost undetectable following biodegradation (Figure 3). Overall, PAR and UV treatments retained
325 the largest proportion of proteinaceous peaks, predominantly due to increased fluorescence of peak T and M.
326

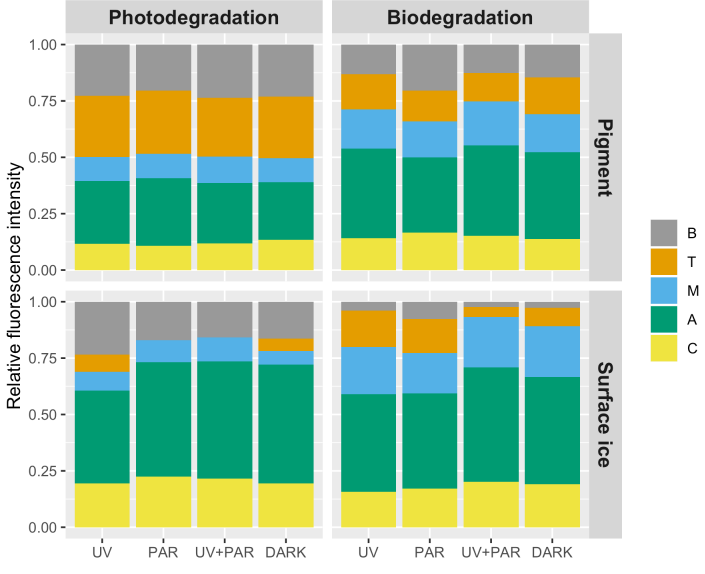

327
328 **Figure 2: The mean relative fluorescence intensity (R.U.; n = 3) associated with commonly identified peaks (B, T, M, A**
329 **and C) in the fluorescence spectra of natural waters (Coble, 1996; Coble et al., 2014) (n=3). Peaks B and T are often**
330 **associated with protein**

https://doi.org/10.5194/bg-2020-227
Preprint. Discussion started: 3 July 2020

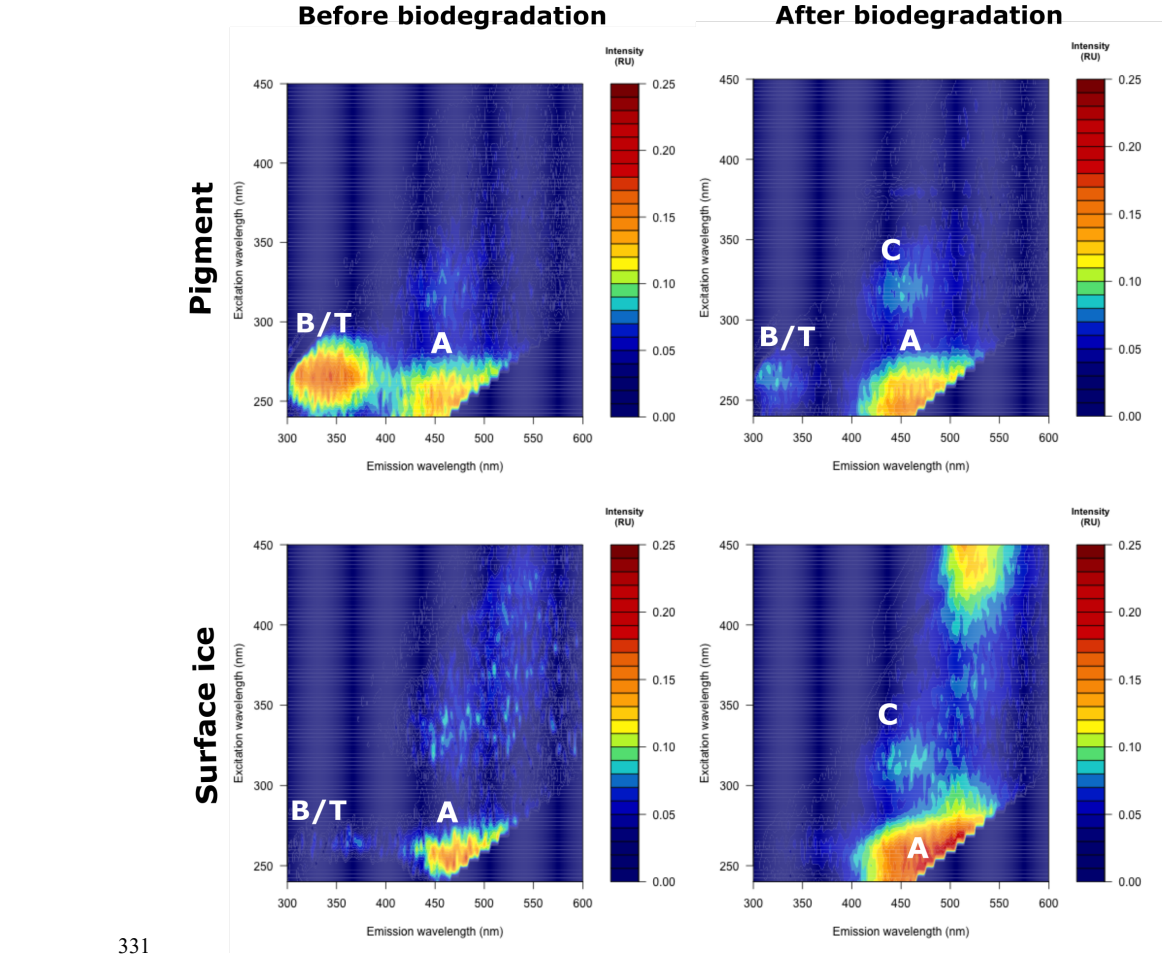

Figure 3: Excitation-Emission matrices (EEMs) for the DARK pigment and surface ice before and after biodegradation. Peaks identified are those typically identified in natural water fluorescence spectra (Birdwell and Engel, 2010; Coble, 1996; Coble et al., 2014). Peaks A and C are generally associated with fluorophores in humic-like DOM whereas peaks B and T are associated with proteinaceous DOM.

The average degree of humification (HIX) across all light treatments in the pigment was 0.51 ± 0.01 which was significantly lower than the surface ice average HIX of 0.57 ± 0.11 ($F_{1,32}$ = 46.8, $p < 0.001$). Following photodegradation, HIX was not significantly different across light treatments for either pigment or surface ice (Figure 4). However, HIX increased significantly by 29 % and 12 % in the pigment and surface ice respectively following biodegradation (pigment: $F_{1,32}$ = 46.8, $p < 0.001$; surface ice $F_{1,32}$ = 46.8, $p < 0.01$). The average fluorescence index (FI) was not significantly different between the pigment (0.51 ± 0.15) and surface ice (0.57 ± 0.11). Following biodegradation, FI of the pigment increased significantly ($F_{1,32}$ = 3.5, $p < 0.05$) whereas surface ice FI remained relatively constant.

https://doi.org/10.5194/bg-2020-227
Preprint. Discussion started: 3 July 2020

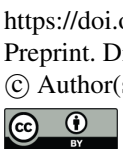

Biogeosciences
Discussions
Open Access
EGU

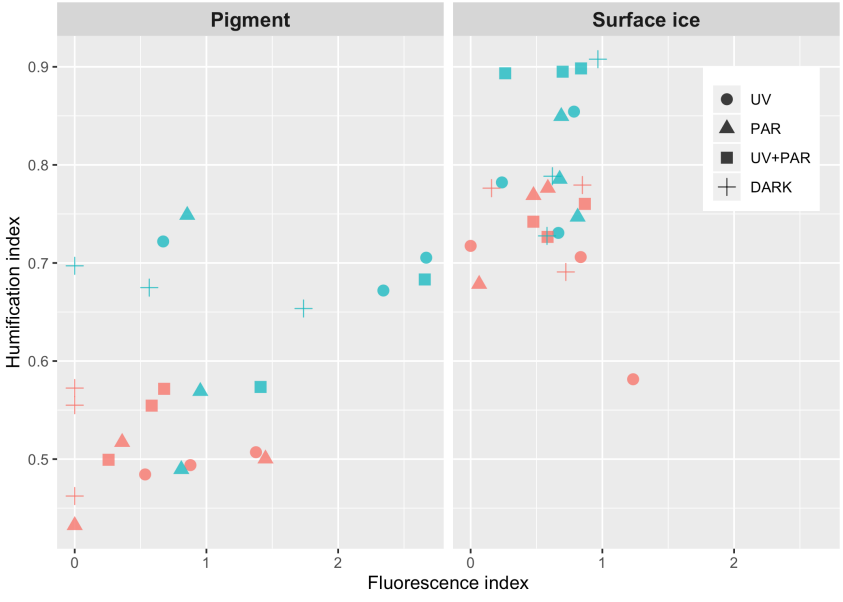

346

347 **Figure 4: Humification index (HIX) against the fluorescence index (FI) for pigment and surface ice after**
348 **photodegradation (red) and after biodegradation (blue) across all light treatments. Increasing HIX indicates the**
349 **presence of more humic compounds. Low FI has been associated with terrestrially derived DOM and high FI with**
350 **microbial DOM.**

351

352 Principal component analysis (PCA) was utilised to summarise all absorbance and fluorescence indices and to
353 elucidate underlying trends of the dataset (Figure 5; Table 4). PC1 described 43 % of the variance in the data and
354 shows strong positive loadings for parameters associated with high molecular weight, aromatic compounds (peak
355 M fluorescence intensity, $SUVA_{365}$ and peak A intensity; Table 4). PC2 accounted for 23 % of the variance and
356 represented Specific visible absorbance at λ440 (SVA_{440}), spectral slope between 300 - 700 nm ($S_{300-700}$) and
357 $SUVA_{254}$. There were no significant differences in PC1 or PC2 between light treatments; however, carbon source
358 (i.e. pigment or surface ice) and type of degradation (i.e. photodegradation or biodegradation) were found to be
359 significant drivers of change in PC1 ($F_{1,46} = 31.8$, $p < 0.001$; $F_{1,46} = 35.6$, $p < 0.001$ respectively) and PC2 ($F_{1,46} =$
360 48.7, $p < 0.001$; $F_{1,46} = 18.9$, $p < 0.001$ respectively).

361

362

https://doi.org/10.5194/bg-2020-227
Preprint. Discussion started: 3 July 2020

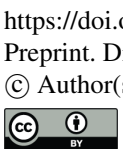

Biogeosciences
Discussions
Open Access
EGU

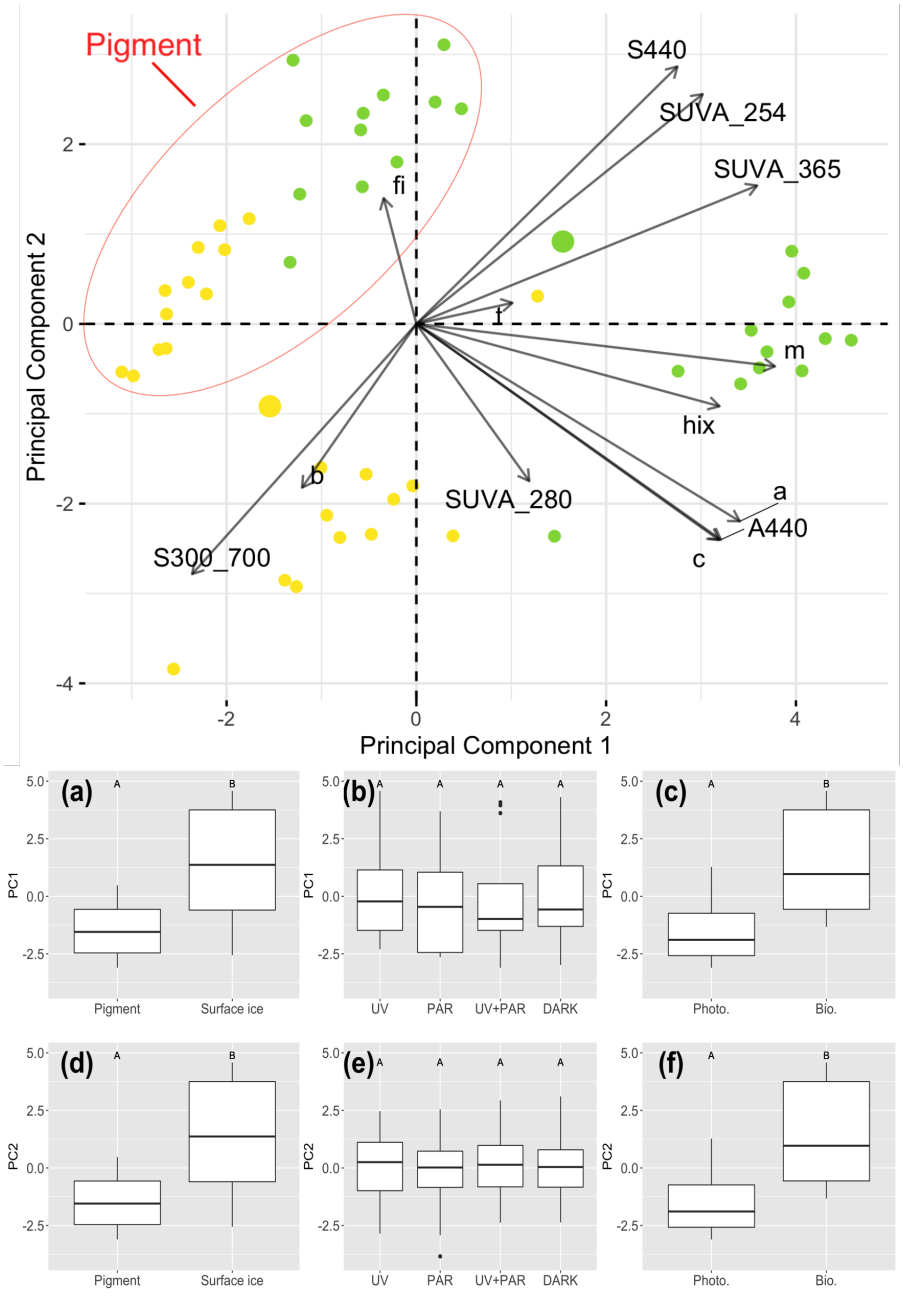

Figure 5: Principle component analysis (PCA) of the absorbance and fluorescence for photodegraded (yellow) or biodegraded (green) DOM. Points representing pigment DOM are circled in red and the remaining points represent surface ice DOM. PC1 accounts for 43 % and PC2 accounts for 23 % of the variability in the dataset. Absorbance indices include SUVA254, SUVA280, SUVA365, A440, spectral slope between 300 – 700 nm (S300_700) and fluorescence indices include fluorescence intensity of peaks B, T, M, A, C, humification index (HIX) and fluorescence index (FI). Boxplots of PC1 against carbon source (a), light (b) and degradation type (i.e. photodegradation or biodegradation; c) and PC2 against carbon source (d), light (e) and degradation type (f). Letters denote significant differences between groups ($p < 0.05$)

https://doi.org/10.5194/bg-2020-227
Preprint. Discussion started: 3 July 2020

372 **Table 4: Component loadings of PCA analysis of absorbance and fluorescence indices. The largest component loading**
373 **is highlighted in grey. Absorbance indices include SUVA254, SUVA280, SUVA365, A440, spectral slope between 300 –**
374 **700 nm (S300_700) and fluorescence indices include fluorescence intensity of peaks B, T, M, A, C, humification index**
375 **(HIX) and fluorescence index (FI).**

	PC1	PC2	PC3
Proportion of variance	42.7 %	22.7 %	10.1 %
Cumulative proportion	42.7 %	65.4 %	75.5 %
Component loadings			
B	-0.12	-0.26	0.28
T	0.10	0.03	0.63
M	0.39	-0.07	0.07
A	0.35	-0.31	-0.04
C	0.33	-0.34	-0.01
FI	-0.04	0.20	-0.51
HIX	0.33	-0.13	-0.45
$S_{300-700}$	-0.24	-0.39	-0.09
$SUVA_{254}$	0.31	0.36	0.05
$SUVA_{280}$	0.12	-0.25	0.18
$SUVA_{365}$	0.37	0.22	0.09
SVA_{440}	0.28	0.40	0.07
A_{440}	0.33	-0.34	-0.07

376

377 ### 3.2 DOC quantity

378 Average dissolved organic carbon (DOC) concentration of the DARK pigment was 2.5 ± 0.04 mg L^{-1} and
379 photodegradation did not significantly alter concentrations in the UV, PAR or UV+PAR treatments. During the
380 31-days of biodegradation, DOC concentrations in the DARK treatment exhibited high levels of variability and
381 by the end of the incubation period had decreased by ~ 0.25 mg L^{-1}, but this was not significant (Figure 6).
382 Concentrations across light treatments were equally variable decreasing by ~ 1 mg L^{-1} over 31 days; however,
383 were not significantly different from DARK. The percent of biodegradable DOC (%BDOC) was ~ 10 % and was
384 not significantly different between UV and PAR exposed and DARK pigment (Appendix A; Table A1). The
385 addition of nutrients (+Nutrients) to incubations did not affect the DOC concentration across any of the light
386 treatments; however, overall %BDOC in +Nutrients was significantly higher than the normal incubations ($F_{1,61}$ =
387 8.7, $p < 0.01$; Appendix A).
388

https://doi.org/10.5194/bg-2020-227
Preprint. Discussion started: 3 July 2020

Biogeosciences
Discussions
Open Access
EGU

389 The average DOC concentration (19.1 ± 0.03 mg L^{-1}) in the DARK surface ice was ~ 8 times greater than in the
390 pigment and no significant change in concentration was found across light treatments following photodegradation.
391 Nevertheless, DOC concentrations did decrease significantly during biodegradation incubations across all light
392 treatments ($F_{5,212} = 432$, $p < 0.001$). DOC concentrations in DARK were significantly lower than in other light
393 treatments at 6 days ($F_{3,36} = 41.4$, $p < 0.01$ for all) and 10 days ($F_{3,36} = 32.9$, $p < 0.001$ for all). The UV, PAR and
394 UV+PAR treatments followed similar trajectories during the incubation period; however, only the DOC
395 concentration in the UV treatment was significantly higher than in DARK at 31 days ($F_{3,36} = 4.7$, $p < 0.01$). The
396 BDOC of surface ice was ~ 30 % and was significantly higher than the pigment ($F_{1,61} = 839$, $p < 0.001$); however,
397 there was no significant difference across light treatments (Appendix A). The DOC concentration in the normal
398 treatment was not significantly different from the +Nutrients treatments following biodegradation.
399

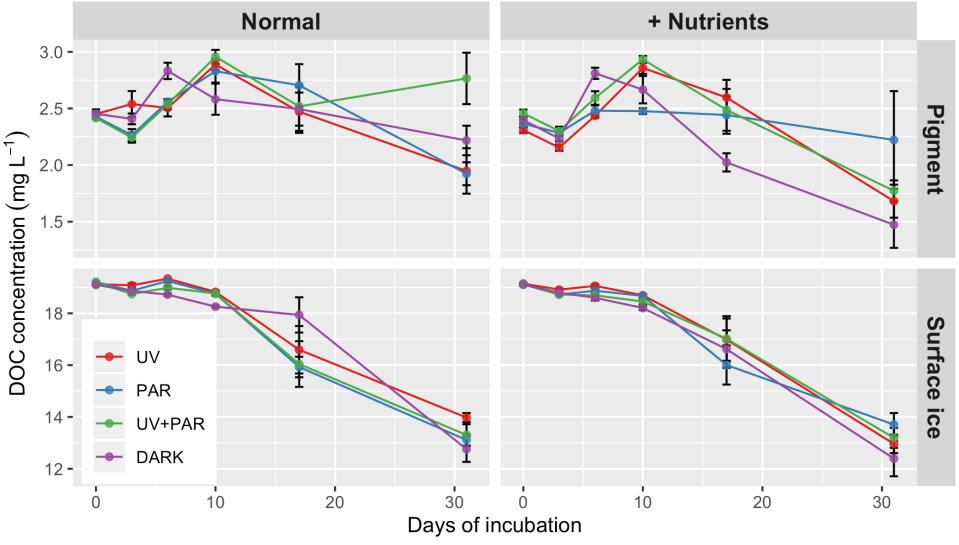

400
401 **Figure 6: Dissolved organic carbon (DOC) concentration (mg L-1) during the 31-day biodegradation period in the**
402 **normal and nutrient addition (+Nutrients) incubations for the pigment and surface ice (mean ± SE, n = 5).**

403

404 ### 3.3 Bacterial abundance and growth efficiency

405 Bacterial abundance in pigment incubations did not increase significantly over the 31-day incubation period across
406 any of the light treatments (Figure 7). Indeed, when normalised against the change in bacterial abundance in the
407 Milli-Q control, abundance actually decreased in the PAR, UV+PAR and DARK treatments during the incubation
408 period. In the +Nutrients treatment, abundance increased in the UV, PAR and DARK treatments to 0.7 ± 0.2 x10^6
409 cells mL^{-1}; however, this was not significant. Average bacterial growth efficiency (BGE) for all pigment
410 treatments was < 4 % and substantial variability was observed across light and nutrient treatments (Appendix A).
411
412 In contrast to the pigment incubations, bacterial abundance across all surface ice treatments increased significantly
413 between 3 and 9-fold during the incubation period ($F_{3,61} = 18.4$, $p < 0.001$). At 17 days, the largest increases were
414 observed in the UV and UV+PAR treatments which supported an abundance of 2.0 ± 1.1 x10^6 cells mL^{-1} and 1.7

https://doi.org/10.5194/bg-2020-227
Preprint. Discussion started: 3 July 2020

± 0.3 x10^6 cells mL^{-1} respectively. Rapid growth in PAR-irradiated surface ice was observed in the final 14 days and as such the final abundance of 9.0 ± 1.7 x10^6 cells mL^{-1} was significantly larger than DARK ($F_{3,61}$ = 2.2, $p < 0.05$). Average abundance at the end of biodegradation across all light treatments was 4.7 ± 1.5 x10^6 cells mL^{-1} and was not significantly different in the +Nutrients treatment. Average BGE in the surface ice was 6.7 ± 1.3 % which was significantly higher than the pigment ($F_{1,31}$ = 4.7, $p < 0.05$). However, BGE was not significantly different across light or nutrient treatments (Appendix A).

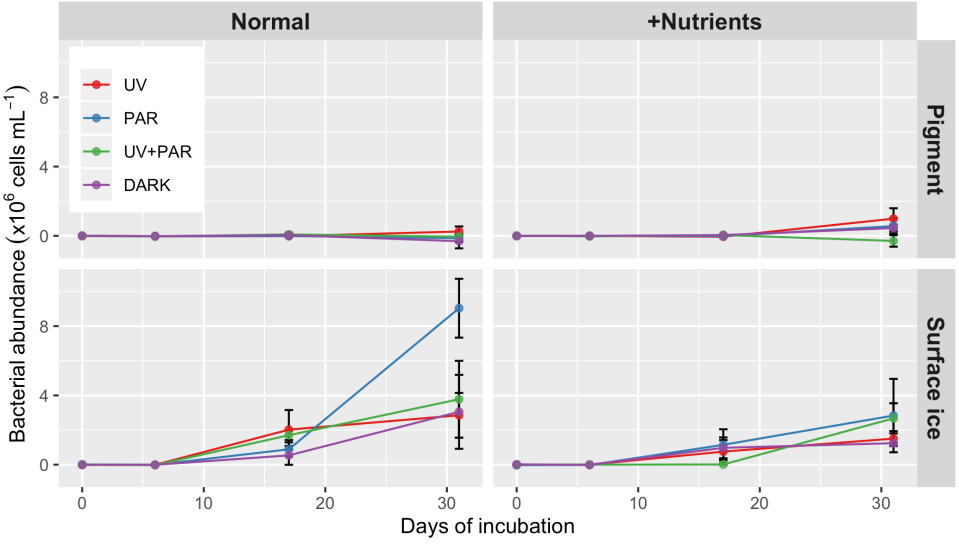

Figure 7: Bacterial abundance in pigment and surface ice coloured by light treatment across the nutrient and nutrient addition (+Nutrients) incubations (mean ± SE, n = 3)

4 Discussion

Active microbial communities store and transform carbon across the Greenland Ice Sheet (GrIS) supraglacial environment. Glacier algae residing within the surface ice contain a dark coloured photoprotective pigment, which comprises a large proportion of the cell (~ 4 % of the dry weight) (Remias et al., 2012; Williamson et al., 2020), and may thus represent a vast source of carbon. Glacier algae are responsible for the majority of carbon fixation within the surface ice (Williamson et al., 2018; Yallop et al., 2012), which is an essential autochthonous carbon source for heterotrophic bacterial communities (Nicholes et al., 2019; Yallop et al., 2012). Despite the surface ice receiving extremely high levels of irradiation, the role of photodegradation on carbon flows was yet to be constrained. This study assessed responses in the composition and quantity of glacier algae secondary pigment and surface ice DOM sources following exposure to UV, PAR, UV+PAR (photodegradation) and subsequent incubation with bacterial communities isolated from the ambient environment (biodegradation). Our results indicate that the composition of algal pigment and surface ice DOM is altered following exposure to radiation, but that the quantity of DOC remains constant. Biodegradation caused the greatest changes to DOM composition and DOC quantity, particularly for surface ice DOM sources.

https://doi.org/10.5194/bg-2020-227
Preprint. Discussion started: 3 July 2020


Biogeosciences
Discussions
Open Access
EGU

4.1 Glacier algal phenolic pigment

The secondary phenolic pigment extracted from glacier algae exhibited absorbance that was highly comparable with previous characterisations of this substance, displaying strong absorption particularly over UV-A and UV-B wavelengths, which decreased across the visible spectrum (Remias et al., 2012; Williamson et al., 2020). Peaks in absorption observed at λ_{285nm}, λ_{304nm} and λ_{385nm} likely reflect different moieties within the pigment structure (Remias et al., 2012; Williamson et al., 2020). For example, peaks at λ_{304nm} and λ_{389nm} have previously been identified as purpurogallin carboxylic acid-6-*O*-β-D-glucopyranoside ($C_{18}H_{18}O_{12}$), which is formed from the chemical oxidation of gallic acid or from a mixture of gallic acid and pyrogallol (Polewski et al., 2002; Remias et al., 2012). Equally, a peak at λ_{278nm} is thought to be gallic acid glycoside and may represent an important biosynthetic precursor to purpurogallin carboxylic acid (Remias et al., 2012). Given the similarity in absorption peaks, it is likely these compounds are also present in the pigment utilised for this experiment. The chemical composition and absorption of pigment likely reflects its primary role of protecting chloroplasts from damaging UV and high energy blue visible radiation, while transmitting longer, less damaging wavelengths for photosynthesis (Williamson et al., 2020).

We observed structural changes to light-sensitive (chromophoric) regions of the glacier algal pigment following exposure to UV radiation; however, the quantity and bioavailability of compounds remained consistent across light treatments. UV-irradiated pigment exhibited a depression in absorption associated with purpurogallin carboxylic acid and gallic acid glycoside, suggesting that these compounds were subject to photodegradation. Ward and Cory (2016) highlighted that carboxylic acids in Arctic algal mats and permafrost were highly susceptible to photodegradation and form a variety of hydrocarbons. The concomitant increase in $SUVA_{254}$ and $SUVA_{365}$ may indicate the transformation into aromatic compounds, which absorb at λ_{254nm} and λ_{365nm} (Uyguner and Bekbolet, 2005; Weishaar et al., 2003). Alternatively, UV radiation may preferentially degrade aliphatic, low molecular weight (LMW) DOM resulting in a greater proportion of aromatic DOM (Ward and Cory, 2016). This is common in other aquatic environments and results in UV radiation effectively reducing the availability of LMW DOM sources to heterotrophic communities (Amado et al., 2015; Ward and Cory, 2016). Despite compositional changes to pigment DOM following UV exposure, bulk DOM quantity remained constant across light treatments. Photosensitive DOM (i.e. CDOM) accounts for only a fraction of the total DOM pool (Fleck et al., 2014), therefore structural alterations can occur without altering the bulk DOM quantity (Cory et al., 2011; Spencer et al., 2007). Given that pigment DOM fluorescence also remained consistent across light treatments, our data are consistent with variation in pigment DOM composition but not quantity following exposure to potential photodegradation.

Biodegradation incubations revealed that certain components of glacier algal pigment may be transformed by the heterotrophic bacterial community. Consistent with previous studies, $SUVA_{254}$ and $SUVA_{365}$ increased across incubations, concomitant with decreasing contributions of proteinaceous fluorescence and suggestive of preferential consumption of LMW aliphatic DOM by bacterial communities (Antony et al., 2018; Hansen et al., 2016; Kirchman, 2003). Most notably, reduced absorption associated with purpurogallin carboxylic acid and gallic acid glycoside indicates that these compounds may comprise a proportion of the bioavailable substrates consumed by the bacterial community. Carboxylic acids have been observed to be readily assimilated into bacterial biomass, thus these compounds are considered largely bioavailable (Bertilsson and Tranvik, 1998).

https://doi.org/10.5194/bg-2020-227
Preprint. Discussion started: 3 July 2020

Interestingly, irradiated pigment retained greater purpurogallin carboxylic acid and gallic acid glycoside absorption compared to DARK treatments, highlighting that UV and PAR exposure either reduces the bioavailability of these compounds or produces more bioavailable compounds that are preferentially consumed (Amado et al., 2015; Lindell et al., 1995; Zepp and Moran, 1997). The humification (HIX) of pigment and the dominance of peak M indicated the production of LMW, humic DOM that is widely attributed to biological activity (Coble, 1996; Murphy et al., 2008). This is corroborated by the increased FI following biodegradation confirming a greater dominance of DOM of a microbial origin (McKnight et al., 2001). Overall, biodegradation incubations revealed the potential for bacterial communities to transform a small proportion of bioavailable carbon (~ 10 %) sourced from glacier algal secondary pigment and demonstrated that UV degradation may influence which DOM components are degraded.

Despite the marked changes in DOM composition following biodegradation, our results indicated that only ~ 3 % of carbon was incorporated into bacterial biomass and bacterial abundance thus remained relatively constant across all light treatments. This suggests that glacier algal pigment may be a low-quality carbon substrate for surface ice bacterial communities and the overall quality of carbon was not changed by photodegradation. We provide two explanations for this, both related to the polyphenolic nature of purpurogallin carboxylic acid and gallic acid glycoside. Polyphenols represent a variety of chemical substances found in algae and higher plants that have a range of ecological and physiological functions (Bhat et al., 1998; Cannell et al., 1988). Notably, polyphenols have antimicrobial properties and play an essential role in protecting cells against bacterial and fungal pathogens (Cannell et al., 1988; Lima et al., 2016; Nguyen et al., 2013; Scalbert, 1991). A range of bacterial species are susceptible to polyphenol inhibition (Scalbert, 1991; Taguri et al., 2006) and we propose that the majority of the surface ice bacterial community are affected. Despite this, compositional changes to DOM outlined previously may suggest that some resistant species reside within the surface ice environment. Bacterial degradation or modification of polyphenols, as observed in our incubations, has been highlighted as an important mechanism for overcoming inhibition, such as the ability of *Achromobacter sp.* to grow in a gallotannin media (Bhat et al., 1998; Scalbert, 1991; Smith et al., 2005). It is possible that the inhibition of the majority of the bacterial community by the polyphenolic nature of pigment may have resulted in low bacterial growth efficiency.

In addition to the potential inhibition of bacteria by antimicrobial properties of glacier algal phenolic pigment, nutrient limitation may have also restricted bacterial growth. Nitrogen and phosphorus are essential macronutrients obtained by bacteria from both inorganic and organic sources (Dodds, 2010; Sigee, 2004). Organic sources include proteins, nucleic acids and amino acids, which are actively and passively released from cells via extrapolymeric substances and cell lysis (Sigee, 2004). Both purpurogallin carboxylic acid and gallic acid glycoside do not contain nitrogen or phosphorus and hence are easily synthesised in high light, low nitrogen environments, such as supraglacial surface ice (Remias et al., 2009, 2012). Accordingly, organic nutrient sources were likely very limited in the pigment incubations, potentially restricting bacterial activity, driving utilisation of ~ 20 % of carbon. In contrast, incubations spiked with nitrogen and phosphorus (+Nutrients) exhibited much greater bacterial growth and a ~ 10 % increased BDOC, thus additional nutrients likely facilitated a greater exploitation of carbon sources.

https://doi.org/10.5194/bg-2020-227
Preprint. Discussion started: 3 July 2020

520 Although glacier algal secondary pigment could represent a substantial carbon source within the surface ice during
521 bloom events, the mechanism of pigment release remains unconstrained. Given the metabolic cost of producing
522 this secondary pigment and its essential role protecting the cell from photodamage, it is unlikely to be actively
523 excreted by glacier algae. Alternative mechanisms of release may include passive leakage or lysis of cells due to
524 natural senescence or viral/fungal attack (Dodds, 2010; Sigee, 2004; Zlotnik and Dubinsky, 1989); however, the
525 degree of leakage and mortality rate of glacier algae remains unconstrained. Overall, biodegradation incubations
526 revealed that glacier algal phenolic pigment is largely unavailable to heterotrophic bacterial communities from
527 the surface ice of the GrIS. Despite this, algal pigment may represent a viable carbon source for Archaea or fungi
528 within the surface ice community and further investigation is therefore required to reveal the fate of this carbon
529 source.
530

531 **4.2 Surface ice DOM**

532 To the best of our knowledge, this is the first spectroscopic characterisation of surface ice DOM from the Dark
533 Zone of the Greenland Ice Sheet. Our results highlight remarkable similarities in absorption characteristics
534 between surface ice and pigment DOM indicating the presence of purpurogallin carboxylic acid and gallic acid
535 glycoside in surface ice. This may be a result of natural glacier algal cell lysis; however, we also acknowledge
536 that algal cells may have lysed during experimental set up, releasing pigment and thus further *in situ* investigations
537 are required to clarify whether this is representative. Despite this, purpurogallin carboxylic acid and gallic acid
538 glycoside were some of the most strongly light absorbing compounds, therefore the release of even small
539 concentrations of pigment to the ambient environment could substantially alter the optical properties of surface
540 meltwater. Surface ice DOM exhibited predominantly humic-like fluorescence dominated by peaks A and C; both
541 of which are often associated with the presence of HMW, aromatic DOM of terrestrial plant or soil origin (Coble,
542 1996; Coble et al., 1990; Fellman et al., 2010). This is surprising given the high levels of primary production by
543 glacier algae reported from the surface ice (Williamson et al., 2018; Yallop et al., 2012) and the relatively low
544 input of carbon from allochthonous sources in our sampling region on the GrIS (Stibal et al., 2012). However,
545 peaks A and C have also been observed following bacterial degradation of autochthonous DOM (Stedmon and
546 Markager, 2005) and it is therefore possible that surface ice DOM had already undergone a degree of
547 biodegradation prior to sampling. Equally, the formation of humic-like DOM following photodegradation of algal-
548 derived DOM is widely reported (Amado et al., 2015; Stefan et al., 2000; Tranvik and Kokalj, 1998). Carbon
549 transformation and cycling within the surface ice is thus highly dynamic, with rapid production and consumption
550 of bioavailable compounds via biotic and abiotic processes.
551

552 The exposure of surface ice to UV and PAR radiation resulted in a number of compositional changes to DOM.
553 Purpurogallin carboxylic acid and gallic acid glycoside were susceptible to degradation on exposure to UV
554 radiation and responsible for the major shifts in absorption and SUVA indices. An increased proteinaceous
555 signature dominated by peak B in UV-irradiated surface ice indicated that UV radiation degraded high molecular
556 weight (HMW) humic DOM into smaller, more bioavailable compounds. This is widely reported from other high-
557 light aquatic environments and was found to stimulate bacterial production and growth (Amado et al., 2015;
558 Anesio et al., 2005; Lindell et al., 1995; Zepp and Moran, 1997). Along with UV radiation, PAR was also found

https://doi.org/10.5194/bg-2020-227
Preprint. Discussion started: 3 July 2020

559 to alter the chemical structure of surface ice DOM, with decreased $SUVA_{254}$ and $SUVA_{365}$ representing a lower
560 proportion of aromatic DOM compared to DARK treatment samples. A greater proportion of humic- like
561 fluorescence, characterised by a lack of peak T and a dominant peak M, in PAR- and UV+PAR- irradiated surface
562 ice suggested that proteinaceous DOM is converted to LMW, humic-like DOM by PAR. It is likely that in the
563 UV+PAR treatment, these opposing processes (the degradation and formation of humic-like DOM) are occurring
564 simultaneously, with formation driven by PAR representing the dominant process. This contrasts with the findings
565 of Antony *et al.*, (2018); however, may simply represent the difference in DOM composition between surface ice
566 of the GrIS and snow in Antarctica. Although DOC concentrations were consistent across light treatments, we
567 have demonstrated that surface ice DOM undergoes structural and compositional changes following exposure to
568 UV and PAR.
569
570 Biodegradation incubations revealed that the heterotrophic bacteria community was able to extensively rework
571 surface ice DOM. The DARK surface ice exhibited increased SUVA indices, confirming that bacteria primarily
572 consume aliphatic, LMW compounds (Antony et al., 2018; Hansen et al., 2016; Kirchman, 2003). This was further
573 corroborated by an increase in peak M fluorescence and humification (HIX), highlighting preferential bacterial
574 consumption of proteinaceous surface ice DOM and production of LMW humic-like DOM (Murphy et al., 2008).
575 Although purpurogallin carboxylic acid and gallic acid glycoside were degraded across all treatments, absorption
576 was still evident demonstrating that these compounds were less rigorously degraded than in the pigment
577 incubations. This may indicate that degradation of these compounds is metabolically intensive and comparatively
578 less attractive in the presence of alternative carbon sources. The degradation of these compounds within surface
579 ice DOM supported substantial increases in bacterial abundance throughout incubations. It is likely that the greater
580 diversity of DOM compounds in surface ice provided a plethora of substrates that facilitated growth across a
581 broader range of bacterial species within the community (Antony et al., 2017; Smith et al., 2018). BGE in surface
582 ice was highly comparable with that in glacier forefields (Bradley et al., 2016) and 3-times higher than within
583 supraglacial streams (Foreman et al., 2013). Bacteria are thus capable of assimilating a greater proportion of
584 bioavailable carbon from the surface ice compared to supraglacial streams.
585
586 Following the biodegradation of photodegraded surface ice, substantial variability in absorbance and fluorescence
587 across light treatments was observed, highlighting the impact of photodegradation on bacterial DOM
588 consumption. For example, UV-irradiated surface ice retained the greatest proportion of aromatic DOM, whereas
589 PAR and UV+PAR retained the least. Additionally, UV- and PAR-irradiated surface ice exhibited a greater
590 proteinaceous signature than DARK, indicating that bioavailable DOM was not as readily consumed in these
591 incubations. Bacterial communities in surface ice are genetically diverse (Perini et al., 2019) and as such, are
592 likely capable of consuming a range of substrates (Fernández-Gómez et al., 2013; Kirchman, 2003). Thus, the
593 community may be consuming different DOM components across light treatments and it is possible that
594 genetically distinct communities develop as a result (Mahmoudi et al., 2017; Smith et al., 2018). We also observed
595 much greater increases in bacterial abundance in irradiated surface ice between 6 and 17 days of incubation
596 compared to DARK. Solar radiation has been observed to increase nitrogen, sulphur and phosphorus
597 bioavailability in organic compounds (Antony et al., 2018) and the formation of inorganic nitrogen on exposure
598 to UV radiation has been widely reported (Bushaw et al., 1996; Wang et al., 2000; Xie et al., 2012). Irradiated

https://doi.org/10.5194/bg-2020-227
Preprint. Discussion started: 3 July 2020

599 surface ice may have contained a greater nutrient concentration that stimulated more rapid bacterial growth.
600 Despite this, the quantity of carbon consumed by bacteria did not differ across light treatments indicating that
601 consumption may be limited by a factor other than DOM composition, such as temperature; however, further
602 research is required to understand this. Our results therefore indicate that although photodegradation does alter
603 DOM composition, bacteria in the surface ice are adept at utilising a range of carbon sources to facilitate growth.
604

605 **5 Conclusions**

606 The results from this study reveal the complex interaction between photodegradation and biodegradation in
607 altering the composition and quantity of secondary phenolic pigment (purpurogallin carboxylic acid-6-*O*-β-D-
608 glucopyranoside) extracted from glacier algae and surface ice DOM. Both carbon sources are susceptible to
609 photodegradation, particularly on exposure to UV radiation, which caused the largest compositional changes to
610 DOM. This is especially important given the potential for ozone holes over the Arctic and subsequent extreme
611 levels of UV radiation that may result (Manney et al., 2011). Our results indicate that glacier algae secondary
612 phenolic pigment contains components that can be degraded by surface ice bacterial communities; however,
613 degradation may be metabolically intensive and therefore pigment is likely not the primary source of carbon
614 within this system. We also hypothesise that glacier algal pigment may exhibit antimicrobial properties which
615 inhibit the growth of specific bacterial species. In contrast, surface ice DOM supported extensive bacterial growth
616 likely due to the wider variety of DOM compounds available. Despite compositional changes to both glacier algal
617 phenolic pigment and surface ice DOM following photodegradation, we did not observe any difference in
618 consumption by the bacteria community suggesting that the bioavailability of DOM was not influenced by
619 exposure to UV or PAR. Photodegradation and biodegradation of surface ice DOM are likely intimately linked
620 within the surface ice habitat and act as fundamental controls on the composition and quantity of DOM exported
621 to downstream environments.
622

623 *Data availability*
624 All data is available via the Polar Data Centre (https://www.bas.ac.uk/data/uk-pdc/). DOI TO BE MINTED
625 AFTER REVIEW PROCESS.
626

627 *Team list*
628 The Black and Bloom team comprises of: Martyn Tranter, Alexandre Anesio, Marian Yallop, Christopher
629 Williamson, Ewa Poniecka, Miranda Nicholes, Alexandra Holland, Liane Benning, Jim McQuaid, Stefanie Lutz,
630 Jenine McCutcheon, Andy Hodson, Edward Hanna, Tristram Irvine-Fynn, Joseph Cook, Jonathan Bamber,
631 Andrew Tedstone, Jason Box and Marek Stibal.
632

633 *Author contribution*
634 MN, CW and AA conceived and designed the study. AH aided MN with sampling during the incubation
635 experiment. Sample analysis and data presentation was conducted by MN with supervision from CW, AA, MT
636 and MY. MN wrote the manuscript with inputs from CW and AA, all authors reviewed the final manuscript.

https://doi.org/10.5194/bg-2020-227
Preprint. Discussion started: 3 July 2020

637

638 *Competing interests*

639 The authors declare that they have no conflict of interest.

640

641 *Financial support*

642 This work was funded as part of the UK Natural Environment Research Council Consortium Grant "Black and
643 Bloom" (NE/M021025/1).

644

645 *Acknowledgements*

646 The authors would like to thank the entire Black and Bloom team, especially those involved in the 2017 field
647 season. We also thank Jennifer Maddalena, Helena Pryer, Fotis Sgouridis and Ioanna Petropoulou for their
648 assistance with experimental set up and supporting using laboratory instruments.

649

650 **References**

651 Aiken, G. R.: Fluorescence and dissolved organic matter: A chemist's perspective, in Aquatic Organic Matter
652 Fluorescence, pp. 35–74, Cambridge University Press, Cambridge., 2014.

653 Amado, A. M., Cotner, J. B., Cory, R. M., Edhlund, B. L. and McNeill, K.: Disentangling the Interactions Between
654 Photochemical and Bacterial Degradation of Dissolved Organic Matter: Amino Acids Play a Central Role,
655 Microb. Ecol., 69(3), 554–566, doi:10.1007/s00248-014-0512-4, 2015.

656 Anesio, A. M. and Granéli, W.: Photochemical mineralization of dissolved organic carbon in lakes of differing
657 pH and humic content, Arch. für Hydrobiol., 160(1), 105–116, doi:10.1127/0003-9136/2004/0160-0105, 2004.

658 Anesio, A. M., Graneli, W., Aiken, G. R., Kieber, D. J. and Mopper, K.: Effect of Humic Substance
659 Photodegradation on Bacterial Growth and Respiration in Lake Water, Appl. Environ. Microbiol., 71(10), 6267–
660 6275, doi:10.1128/AEM.71.10.6267-6275.2005, 2005.

661 Antony, R., Willoughby, A. S., Grannas, A. M., Catanzano, V., Sleighter, R. L., Thamban, M., Hatcher, P. G. and
662 Nair, S.: Molecular Insights on Dissolved Organic Matter Transformation by Supraglacial Microbial
663 Communities, Environ. Sci. Technol., 51(8), 4328–4337, doi:10.1021/acs.est.6b05780, 2017.

664 Antony, R., Willoughby, A. S., Grannas, A. M., Catanzano, V., Sleighter, R. L., Thamban, M. and Hatcher, P. G.:
665 Photo-biochemical transformation of dissolved organic matter on the surface of the coastal East Antarctic ice
666 sheet, Biogeochemistry, 141(2), 229–247, doi:10.1007/s10533-018-0516-0, 2018.

667 Baker, A. and Spencer, R. G. M.: Characterization of dissolved organic matter from source to sea using
668 fluorescence and absorbance spectroscopy, Sci. Total Environ., 333(1–3), 217–232,
669 doi:10.1016/j.scitotenv.2004.04.013, 2004.

670 Benner, R. and Kaiser, K.: Biological and photochemical transformations of amino acids and lignin phenols in
671 riverine dissolved organic matter, Biogeochemistry, 102(1), 209–222, doi:10.1007/s10533-010-9435-4, 2011.

672 Bertilsson, S. and Tranvik, L. J.: Photochemically produced carboxylic acids as substrates for freshwater
673 bacterioplankton, Limnol. Oceanogr., 43(5), 885–895, doi:10.4319/lo.1998.43.5.0885, 1998.

674 Bhat, T. K., Singh, B. and Sharma, O. P.: Microbial degradation of tannins - A current perspectiveBhat, T. K., B.
675 Singh, and O. P. Sharma. 1998. Microbial degradation of tannins - A current perspective. Biodegradation 9:343–
676 357., Biodegradation, 9(Graham 1992), 343–357, doi:10.1023/A:1008397506963, 1998.

https://doi.org/10.5194/bg-2020-227
Preprint. Discussion started: 3 July 2020

677 Birdwell, J. E. and Engel, A. S.: Characterization of dissolved organic matter in cave and spring waters using UV-
678 Vis absorbance and fluorescence spectroscopy, Org. Geochem., 41(3), 270–280,
679 doi:10.1016/j.orggeochem.2009.11.002, 2010.
680 Bradley, J. A., Arndt, S., Šabacká, M., Benning, L. G., Barker, G. L., Blacker, J. J., Yallop, M. L., Wright, K. E.,
681 Bellas, C. M., Telling, J., Tranter, M. and Anesio, A. M.: Microbial dynamics in a High Arctic glacier forefield:
682 a combined field, laboratory, and modelling approach, Biogeosciences, 13(19), 5677–5696, doi:10.5194/bg-13-
683 5677-2016, 2016.
684 Bratbak, G. and Dundas, I.: Bacterial dry matter content and biomass estimations, Appl. Environ. Microbiol.,
685 48(4), 755–757, doi:10.1128/aem.48.4.755-757.1984, 1984.
686 Bushaw, K. L., Zepp, R. G., Tarr, M. A., Schulz-Jander, D., Bourbonniere, R. A., Hodson, R. E., Miller, W. L.,
687 Bronk, D. A. and Moran, M. A.: Photochemical release of biologically available nitrogen from aquatic dissolved
688 organic matter, Nature, 381(6581), 404–407, doi:10.1038/381404a0, 1996.
689 Cannell, R. J., Farmer, P. and Walker, J. M.: Purification and characterization of pentagalloylglucose, and alpha-
690 glucosidase inhibitor/antibiotic from the freshwater green alga Spirogyra varians., Biochem. J., 255(3), 937–941,
691 doi:10.1042/bj2550937, 1988.
692 Chin, Y. P., Alken, G. and O'Loughlin, E.: Molecular Weight, Polydispersity, and Spectroscopic Properties of
693 Aquatic Humic Substances, Environ. Sci. Technol., 28(11), 1853–1858, doi:10.1021/es00060a015, 1994.
694 Coble, P. G.: Characterization of marine and terrestrial DOM in seawater using excitation-emission matrix
695 spectroscopy, Mar. Chem., 51(4), 325–346, doi:10.1016/0304-4203(95)00062-3, 1996.
696 Coble, P. G.: Marine optical biogeochemistry: The chemistry of ocean color, Chem. Rev., 107(2), 402–418,
697 doi:10.1021/cr050350+, 2007.
698 Coble, P. G., Green, S. A., Blough, N. V. and Gagosian, R. B.: Characterization of dissolved organic matter in
699 the Black Sea by fluorescence spectroscopy, Nature, 348(6300), 432–435, doi:10.1038/348432a0, 1990.
700 Coble, P. G., Spencer, R. G. M., Baker, A. and Reynolds, D. M.: Aquatic Organic Matter Fluorescence, in Aquatic
701 Organic Matter Fluorescence, pp. 75–122, Cambridge University Press, Cambridge., 2014.
702 Cory, R. M., Boyer, E. W. and McKnight, D. M.: Spectral Methods to Advance Understanding of Dissolved
703 Organic Carbon Dynamics in Forested Catchments, in Forest hydrology and biogeochemistry, Synthesis of past
704 research and future directions, vol. 216, pp. 117–135., 2011.
705 Dodds, W. K.: Freshwater Ecology: Concepts and Environmental Applications of Limnology, 2nd ed., edited by
706 J. H. Thorp, Academic Press, Cambridge, USA. [online] Available from: https://books.google.pt/books?hl=pt-
707 PT&lr=&id=3OR0102I7n4C&oi=fnd&pg=PP1&ots=WTjIRO5-
708 La&sig=jXU5HH_fNz1iUurzLC2pqdUN9Dk&redir_esc=y#v=onepage&q&f=false, 2010.
709 Ducklow, H.: Bacterial production and biomass in Oceans, in Microbial Ecology of the Oceans, edited by D.
710 Kirchman, pp. 1–47, Wiley, New York. [online] Available from:
711 http://web.vims.edu/bio/microbial/kirch_final.pdf, 2000.
712 Fasching, C., Behounek, B., Singer, G. A. and Battin, T. J.: Microbial degradation of terrigenous dissolved organic
713 matter and potential consequences for carbon cycling in brown-water streams, Sci. Rep., 4, 1–7,
714 doi:10.1038/srep04981, 2014.
715 Fellman, J. B., Hood, E. and Spencer, R. G. M.: Fluorescence spectroscopy opens new windows into dissolved
716 organic matter dynamics in freshwater ecosystems: A review, Limnol. Oceanogr., 55(6), 2452–2462,

https://doi.org/10.5194/bg-2020-227
Preprint. Discussion started: 3 July 2020

717 doi:10.4319/lo.2010.55.6.2452, 2010.
718 Fernández-Gómez, B., Richter, M., Schüler, M., Pinhassi, J., Acinas, S. G., González, J. M. and Pedrós-Alió, C.:
719 Ecology of marine bacteroidetes: A comparative genomics approach, ISME J., 7(5), 1026–1037,
720 doi:10.1038/ismej.2012.169, 2013.
721 Fleck, J. A., Gill, G., Bergamaschi, B. A., Kraus, T. E. C., Downing, B. D. and Alpers, C. N.: Concurrent
722 photolytic degradation of aqueous methylmercury and dissolved organic matter, Sci. Total Environ., 484(1), 263–
723 275, doi:10.1016/j.scitotenv.2013.03.107, 2014.
724 Foreman, C. M., Cory, R. M., Morris, C. E., Sanclements, M. D., Smith, H. J., Lisle, J. T., Miller, P. L., Chin, Y.
725 P. and McKnight, D. M.: Microbial growth under humic-free conditions in a supraglacial stream system on the
726 Cotton Glacier, Antarctica, Environ. Res. Lett., 8(3), doi:10.1088/1748-9326/8/3/035022, 2013.
727 Del Giorgio, P. A. and Cole, J. J.: Bacterial growth efficiency in natural aquatic systems, Annu. Rev. Ecol. Syst.,
728 29, 503–541, doi:10.1146/annurev.ecolsys.29.1.503, 1998.
729 Hansen, A. M., Kraus, T. E. C., Pellerin, B. A., Fleck, J. A., Downing, B. D. and Bergamaschi, B. A.: Optical
730 properties of dissolved organic matter (DOM): Effects of biological and photolytic degradation, Limnol.
731 Oceanogr., 61(3), 1015–1032, doi:10.1002/lno.10270, 2016.
732 Helms, J. R., Stubbins, A., Ritchie, J. D., Minor, E. C., Kieber, D. J. and Mopper, K.: Absorption spectral slopes
733 and slope ratios as indicators of molecular weight, source, and photobleaching of chromophoric dissolved organic
734 matter, Limnol. Oceanogr., 53(3), 955–969, doi:10.4319/lo.2008.53.3.0955, 2008.
735 Hodson, A., Anesio, A. M., Tranter, M., Fountain, A., Osborn, M., Priscu, J., Laybourn-Parry, J. and Sattler, B.:
736 Glacial Ecosystems, Ecol. Monogr., 78(1), 41–67, doi:10.1890/07-0187.1, 2008.
737 Holzinger, A. and Lütz, C.: Algae and UV irradiation: Effects on ultrastructure and related metabolic functions,
738 Micron, 37(3), 190–207, doi:10.1016/j.micron.2005.10.015, 2006.
739 Kellerman, A. M., Guillemette, F., Podgorski, D. C., Aiken, G. R., Butler, K. D. and Spencer, R. G. M.: Unifying
740 Concepts Linking Dissolved Organic Matter Composition to Persistence in Aquatic Ecosystems, Environ. Sci.
741 Technol., 52(5), 2538–2548, doi:10.1021/acs.est.7b05513, 2018.
742 Kirchman, D. L.: The Contribution of Monomers and other Low-Molecular Weight Compounds to the Flux of
743 Dissolved Organic Material in Aquatic Ecosystems, Aquat. Ecosyst., 217–241, doi:10.1016/b978-012256371-
744 3/50010-x, 2003.
745 Li, P. and Hur, J.: Utilization of UV-Vis spectroscopy and related data analyses for dissolved organic matter
746 (DOM) studies: A review, Crit. Rev. Environ. Sci. Technol., 47(3), 131–154,
747 doi:10.1080/10643389.2017.1309186, 2017.
748 Lima, V. N., Oliveira-Tintino, C. D. M., Santos, E. S., Morais, L. P., Tintino, S. R., Freitas, T. S., Geraldo, Y. S.,
749 Pereira, R. L. S., Cruz, R. P., Menezes, I. R. A. and Coutinho, H. D. M.: Antimicrobial and enhancement of the
750 antibiotic activity by phenolic compounds: Gallic acid, caffeic acid and pyrogallol, Microb. Pathog., 99, 56–61,
751 doi:10.1016/j.micpath.2016.08.004, 2016.
752 Lindell, M. J., Granéli, W. and Tranvik, L. J.: Enhanced bacterial growth in response to photochemical
753 transformation of dissolved organic matter, Limnol. Oceanogr., 40(1), 195–199, doi:10.4319/lo.1995.40.1.0195,
754 1995.
755 Mahmoudi, N., Beaupré, S. R., Steen, A. D. and Pearson, A.: Sequential bioavailability of sedimentary organic
756 matter to heterotrophic bacteria, Environ. Microbiol., 19(7), 2629–2644, doi:10.1111/1462-2920.13745, 2017.

https://doi.org/10.5194/bg-2020-227
Preprint. Discussion started: 3 July 2020

757 Manney, G. L., Santee, M. L., Rex, M., Livesey, N. J., Pitts, M. C., Veefkind, P., Nash, E. R., Wohltmann, I.,
758 Lehmann, R., Froidevaux, L., Poole, L. R., Schoeberl, M. R., Haffner, D. P., Davies, J., Dorokhov, V., Gernandt,
759 H., Johnson, B., Kivi, R., Kyrö, E., Larsen, N., Levelt, P. F., Makshtas, A., McElroy, C. T., Nakajima, H.,
760 Parrondo, M. C., Tarasick, D. W., Von Der Gathen, P., Walker, K. A. and Zinoviev, N. S.: Unprecedented Arctic
761 ozone loss in 2011, Nature, 478(7370), 469–475, doi:10.1038/nature10556, 2011.
762 McKnight, D. M., Boyer, E. W., Westerhoff, P. K., Doran, P. T., Kulbe, T. and Andersen, D. T.:
763 Spectrofluorometric characterization of dissolved organic matter for indication of precursor organic material and
764 aromaticity, Limnol. Oceanogr., 46(1), 38–48, doi:10.4319/lo.2001.46.1.0038, 2001.
765 Murphy, K. R., Stedmon, C. A., Waite, T. D. and Ruiz, G. M.: Distinguishing between terrestrial and
766 autochthonous organic matter sources in marine environments using fluorescence spectroscopy, Mar. Chem.,
767 108(1–2), 40–58, doi:10.1016/j.marchem.2007.10.003, 2008.
768 Musilova, M., Tranter, M., Wadham, J., Telling, J., Tedstone, A. and Anesio, A. M.: Microbially driven export
769 of labile organic carbon from the Greenland ice sheet, Nat. Geosci., 10(5), 360–365, doi:10.1038/ngeo2920, 2017.
770 Nguyen, D. M. C., Seo, D. J., Lee, H. B., Kim, I. S., Kim, K. Y., Park, R. D. and Jung, W. J.: Antifungal activity
771 of gallic acid purified from Terminalia nigrovenulosa bark against Fusarium solani, Microb. Pathog., 56, 8–15,
772 doi:10.1016/j.micpath.2013.01.001, 2013.
773 Nicholes, M. J., Williamson, C. J., Tranter, M., Holland, A., Poniecka, E., Yallop, M. L. and Anesio, A.: Bacterial
774 Dynamics in Supraglacial Habitats of the Greenland Ice Sheet, Front. Microbiol., 10(July),
775 doi:10.3389/fmicb.2019.01366, 2019.
776 Ohno, T.: Fluorescence inner-filtering correction for determining the humification index of dissolved organic
777 matter, Environ. Sci. Technol., 36(4), 742–746, doi:10.1021/es0155276, 2002.
778 Perini, L., Gostinčar, C., Anesio, A. M., Williamson, C., Tranter, M. and Gunde-Cimerman, N.: Darkening of the
779 Greenland Ice Sheet: Fungal Abundance and Diversity Are Associated With Algal Bloom, Front. Microbiol.,
780 10(March), 1–14, doi:10.3389/fmicb.2019.00557, 2019.
781 Polewski, K., Kniat, S. and Sławińska, D.: Gallic acid, a natural antioxidant, in aqueous and micellar environment:
782 spectroscopic studies, Curr. Top. Biophys., 26(2), 217–227 [online] Available from:
783 https://www.researchgate.net/publication/284542596, 2002.
784 Pucher, M., Wünsch, U., Weigelhofer, G., Murphy, K., Hein, T. and Graeber, D.: StaRdom: Versatile software
785 for analyzing spectroscopic data of dissolved organic matter in R, Water (Switzerland), 11(11), 1–19,
786 doi:10.3390/w11112366, 2019.
787 Ravanat, J., Douki, T. and Cadet, J.: Direct and indirect effects of UV radiation on DNA and its components, J.
788 Photochem. Photobiol. B Biol., 63(1–3), 88–102, doi:10.1016/S1011-1344(01)00206-8, 2001.
789 Remias, D., Holzinger, A. and Lütz, C.: Physiology, Ultrastructure and Habitat of the Ice Alga Mesotaenium
790 berggrenii (Zygnemaphyceae, Chlorophyta) from Glaciers in the European Alps, Phycologia, 48(4), 302–312,
791 doi:10.2216/08-13.1, 2009.
792 Remias, D., Schwaiger, S., Aigner, S., Leya, T., Stuppner, H. and Lütz, C.: Characterization of an UV- and VIS-
793 absorbing, purpurogallin-derived secondary pigment new to algae and highly abundant in Mesotaenium berggrenii
794 (Zygnematophyceae, Chlorophyta), an extremophyte living on glaciers, FEMS Microbiol. Ecol., 79(3), 638–648,
795 doi:10.1111/j.1574-6941.2011.01245.x, 2012.
796 Scalbert, A.: Antimicrobial properties of tannins, Phytochemistry, 30(12), 3875–3883, doi:10.1016/0031-

https://doi.org/10.5194/bg-2020-227
Preprint. Discussion started: 3 July 2020

9422(91)83426-L, 1991.

Sigee, D. C.: Freshwater Microbiology, John Wiley & Sons, Ltd, Chichester, UK., 2004.

Smith, A. H., Zoetendal, E. and Mackie, R. I.: Bacterial mechanisms to overcome inhibitory effects of dietary tannins, Microb. Ecol., 50(2), 197–205, doi:10.1007/s00248-004-0180-x, 2005.

Smith, H. J., Dieser, M., McKnight, D. M., SanClements, M. D. and Foreman, C. M.: Relationship between dissolved organic matter quality and microbial community composition across polar glacial environments, FEMS Microbiol. Ecol., 94(7), 1–10, doi:10.1093/femsec/fiy090, 2018.

Spencer, R. G. M., Pellerin, B. A., Bergamaschi, B. A., Downing, B. D., Kraus, T. E. C., Smart, D. R., Dahlgren, R. A. and Hernes, P. J.: Diurnal variability in riverine dissolved organic matter composition determined byin situ optical measurement in the San Joaquin River (California, USA), Hydrol. Process., 21(23), 3181–3189, doi:10.1002/hyp.6887, 2007.

Stedmon, C. A. and Markager, S.: Tracing the production and degradation of autochthonous fractions of dissolved organic matter by fluorescence analysis, Limnol. Oceanogr., 50(5), 1415–1426, doi:10.4319/lo.2005.50.5.1415, 2005.

Stefan, B., J., T. L., Bertilsson, S. and Tranvik, L. J.: Photochemical transformation of dissolved organic matter in lakes, Limnol. Oceanogr., 45(4), 753–762, doi:10.4319/lo.2000.45.4.0753, 2000.

Stibal, M., Šabacká, M. and Žárský, J.: Biological processes on glacier and ice sheet surfaces, Nat. Geosci., 5(11), 771–774, doi:10.1038/ngeo1611, 2012.

Stibal, M., Gözdereliler, E., Cameron, K. A., Box, J. E., Stevens, I. T., Gokul, J. K., Schostag, M., Zarsky, J. D., Edwards, A., Irvine-Fynn, T. D. L. and Jacobsen, C. S.: Microbial abundance in surface ice on the Greenland Ice Sheet, Front. Microbiol., 6(MAR), 1–12, doi:10.3389/fmicb.2015.00225, 2015.

Taguri, T., Tanaka, T. and Kouno, I.: Antibacterial spectrum of plant polyphenols and extracts depending upon hydroxyphenyl structure, Biol. Pharm. Bull., 29(11), 2226–2235, doi:10.1248/bpb.29.2226, 2006.

Tranvik, L. and Kokalj, S.: Decreased biodegradability of algal DOC due to interactive effects of UV radiation and humic matter, Aquat. Microb. Ecol., 14(2), 301–307, doi:10.3354/ame014301, 1998.

Tranvik, L. J. and Bertilsson, S.: Contrasting effects of solar UV radiation on dissolved organic sources for bacterial growth, Ecol. Lett., 4(5), 458–463, doi:10.1046/j.1461-0248.2001.00245.x, 2001.

Uyguner, C. S. and Bekbolet, M.: Implementation of spectroscopic parameters for practical monitoring of natural organic matter, Desalination, 176(1-3 SPEC. ISS.), 47–55, doi:10.1016/j.desal.2004.10.027, 2005.

Wang, W., Tarr, M. A., Bianchi, T. S. and Engelhaupt, E.: Ammonium photoproduction from aquatic humic and colloidal matter, Aquat. Geochemistry, 6(3), 275–292, doi:10.1023/A:1009679730079, 2000.

Ward, C. P. and Cory, R. M.: Complete and Partial Photo-oxidation of Dissolved Organic Matter Draining Permafrost Soils, Environ. Sci. Technol., 50(7), 3545–3553, doi:10.1021/acs.est.5b05354, 2016.

Weishaar, J. L., Aiken, G. R., Bergamaschi, B. A., Fram, M. S., Fujii, R. and Mopper, K.: Evaluation of specific ultraviolet absorbance as an indicator of the chemical composition and reactivity of dissolved organic carbon, Environ. Sci. Technol., 37(20), 4702–4708, doi:10.1021/es030360x, 2003.

Williamson, C. J., Anesio, A. M., Cook, J., Tedstone, A., Poniecka, E., Holland, A., Fagan, D., Tranter, M. and Yallop, M. L.: Ice algal bloom development on the surface of the Greenland Ice Sheet, FEMS Microbiol. Ecol., 94(3), 1–10, doi:10.1093/femsec/fiy025, 2018.

Williamson, C. J., Cook, J., Tedstone, A., Yallop, M., McCutcheon, J., Poniecka, E., Campbell, D., Irvine-Fynn,

https://doi.org/10.5194/bg-2020-227
Preprint. Discussion started: 3 July 2020

837 T., McQuaid, J., Tranter, M., Perkins, R. and Anesio, A.: Algal photophysiology drives darkening and melt of the
838 Greenland Ice Sheet, Proc. Natl. Acad. Sci., 201918412, doi:10.1073/pnas.1918412117, 2020.
839 Xie, H., Bélanger, S., Song, G., Benner, R., Taalba, A., Blais, M., Lefouest, V., Tremblay, J.-É. and Babin, M.:
840 Photoproduction of ammonium in the Southeastern Beaufort Sea and its biogeochemical implications,
841 Biogeosciences Discuss., 9(4), 4441–4482, doi:10.5194/bgd-9-4441-2012, 2012.
842 Yallop, M. L., Anesio, A. M., Perkins, R. G., Cook, J., Telling, J., Fagan, D., MacFarlane, J., Stibal, M., Barker,
843 G., Bellas, C., Hodson, A., Tranter, M., Wadham, J. and Roberts, N. W.: Photophysiology and albedo-changing
844 potential of the ice algal community on the surface of the Greenland ice sheet, ISME J., 6(12), 2302–2313,
845 doi:10.1038/ismej.2012.107, 2012.
846 Zepp, R. G. and Moran, M. A.: Role of Photoreactions in the Formation of Biologically Labile Compounds from
847 Dissolved Organic Matter, Limnol. Oceanogr., 42(6), 1307–1316, 1997.
848 Zlotnik, I. and Dubinsky, Z.: The effect of light and temperature on DOC excretion by phytoplankton, Limnol.
849 Oceanogr., 34(5), 831–839, doi:10.4319/lo.1989.34.5.0831, 1989.
850

https://doi.org/10.5194/bg-2020-227
Preprint. Discussion started: 3 July 2020

6 Appendices

Appendix A

Table A1: Bioavailable DOC (BDOC; %) and bacterial growth efficiency (BGE; %) for the pigment and surface ice across light treatments and in the normal and +nutrient treatments (mean ± SE, n=5 for BDOC and n=3 for BGE). Significant differences were only found in %BDOC for pigment across light treatments per nutrient treatment (i.e. normal or +Nutrients) denoted lower case letters and between nutrient treatments per carbon source, denoted by upper case letters.

Carbon source	Light	BDOC (%)		BGE (%)	
		Normal	+ Nutrients	Normal	+ Nutrients
Pigment	UV	^{a}21 ± 8.1 ^{A}	^{ab}27 ± 6.0 ^{A}	2.9 ± 3.7	7.9 ± 4.1
	PAR	^{a}21 ± 4.2 ^{A}	^{a}6.4 ± 17 ^{A}	1.9 ± 1.4	3.1 ± 1.1
	UV+PAR	^{b}0 ^{A}	^{ab}28 ± 3.0 ^{B}	7.8 ± 2.7	2.4 ± 1.4
	DARK	^{ab}9.3 ± 6.2 ^{A}	^{b}39 ± 8.6 ^{B}	0.1 ± 1.3	3.4 ± 2.5
Surface ice	UV	27 ± 0.9	32 ± 1.8	2.3 ± 0.8	4.1 ± 1.2
	PAR	33 ± 1.2	30 ± 2.3	11 ± 0.6	5.8 ± 2.8
	UV+PAR	31 ± 2.3	31 ± 2.0	7.0 ± 2.3	13 ± 7.2
	DARK	33 ± 2.5	35 ± 3.5	6.7 ± 2.5	3.5 ± 0.6